University of Alberta

GROWTH OF VERTICALLY ALIGNED CARBON NANOTUBES WITH MULTILAYERED CATALYSTS

by

Peter Simiao Wang 

A thesis submitted to the Faculty of Graduate Studies and Research
in partial fulfillment of the requirements for the degree of

Master of Science

in

Micro-Electro-Mechanical Systems (MEMS) and Nanosystems

Department of Electrical and Computer Engineering

Edmonton, Alberta
Fall 2008

Your file Votre référence
ISBN: 978-0-494-47438-9
Our file Notre référence
ISBN: 978-0-494-47438-9

Abstract

Vertically aligned carbon nanotubes (VACNT) have many properties that will enable their eventual use in field emission displays, hydrogen storage and composite materials. In this thesis, vertically aligned carbon nanotubes are grown in a high volume CVD system using C_2H_4 feedstock. A novel multilayered catalyst is established and optimized. All materials in the catalyst play a role in enhancing VACNT growth. The optimized catalyst is able to grow 160 μm of densely packed VACNT at 750°C for 5 min with moderate C_2H_4 flow. A simple gas concentration model is established to examine and explain many interesting growth phenomena observed. Techniques for growing VACNTs on small catalyst pads are proposed. The experimental evidence has also shown that the usual method for calculating VACNT growth rate by dividing the VACNT height by the growth time inaccurately estimates the actual growth rate, especially for short growths.

Acknowledgements

I would like to express my sincerest gratitude to my mother, Xiaoguang Pan, and father, Luping Wang. Even though I have long voiced strong oppositions toward any kind of direct involvements in my study and career, it is the things that you do on the side, your love and care, that have given me the utmost support and carry me onto where I am standing today. I owe absolutely everything to you. My sincerest thanks also go to Liang Wang and Dongxiao Liu. Words cannot nearly describe the magnitude of your influence and contribution toward my success over the years.

I would like to thank Dr. Stephane Evoy and Dr. Kenneth Bosnick for providing supervision and financial support during my Master's degree, giving me the opportunity to study and accomplish in the field of carbon nanotubes. Thanks to the Natural Science and Engineering Research Council of Canada (NSERC), iCore, National Institute for Nanotechnology (NINT) and University of Alberta for the generous financial aid that has kept me from hunger. Thanks to Mike O'Toole and Les Schowalter for offering the much needed help on my cleanroom processes, and fixing up everything that I break. Thanks also go to Daniel Salomon and Julie Qian for assisting me with SEM and TEM.

I would like to thank Dai Lei for the fruitful discussions on carbon nanotubes. Thanks to Michael Lau for being an awesome office neighbor for 2 years. Your uncontrolled consumption of coffee still amazes me. And I would like to thank all of my friends for brightening up many mind-numbing days with joy.

Table of Contents

List of Figures

List of Abbreviations

1 Introduction 1

1.1 Physical Characteristics 3

1.2.1 Electronic Properties 5

1.2.2 Optical Properties 7

1.2.3 Mechanical Properties 7

1.3 Vertically-aligned Carbon Nanotubes 8

2 Carbon Nanotube Growth Methods 10

2.1 Arc discharge 10

2.2 Laser ablation 12

2.3 Chemical vapor deposition 13

2.4 Catalyst Preparation 17

3 Growth of Vertically Aligned Carbon Nanotubes 19

3.1 Catalyst preparation methodology 19

3.2 CNT growth Setup 21

3.3 Procedure 22

4 Catalyst Design 25

4.1 Controlling catalyst size 26

4.2 Catalyst composition 29

4.2.1 Catalyst Material 29

4.3.2 Optimization of the Catalyst 33

5 Discussion 40

5.1 Effects of individual material in the catalyst 40

5.2 Growth on different substrate 46

5.3 Gas concentration effect on CNT growth 47

5.4 Regulation of amorphous carbon formation 51

5.5 When does CNT growth initiate? 54

5.6 Local carbon concentration 56

5.7 Effect of H_2 60
6 Further Directions 61
6.1 Extended Growth 61
6.2 Growth on Small Catalyst Pads 61
6.3 Uniformity 62
6.4 Catalyst Pre-growth Treatment 62
6.5 Water Assisted Growth 63
6.6 Residual Gas Analyzer 63
7 Conclusion 64
References 67

List of Figures

Figure 1: Single-walled and Multi-walled carbon nanotubes 4

Figure 2: Graphene sheet with (n, m) chiral vectors 5

Figure 3: Diagram of an arc discharge setup for CNT growth 11

Figure 4: Diagram of a typical laser ablation chamber 13

Figure 5: Diagram of a chemical vapor deposition setup 14

Figure 6: Diagram illustrating VLS growth mechanism 16

Figure 7: Thickness profile from shutter manipulation 21

Figure 8: SEM images of annealed Fe nanoparticles 27

Figure 9: Particle distribution of annealed Fe 28

Figure 10: CNT growth from individual Fe and Ni catalysts 30

Figure 11: CNT growth from Ni-Fe and Cr-Ni-Fe catalysts 31

Figure 12: CNT growth from Al_2O_3-Cr-Ni-Fe catalyst 32

Figure 13: Graph of VACNT heights grown from varying Cr thicknesses 34

Figure 14: Graph of VACNT height grown from varying Ni thickneses 35

Figure 15: Graph of VACNT height grown from varying Fe thicknesses 36

Figure 16: Graph of VACNT height grown from varying Al2O3 thicknesses 38

Figure 17: Multilayered catalyst design and consequent VACNT growth 39

Figure 18: Phase diagrams of Fe-Ni 41

Figure 19: Fe and Ni-Fe catalytic particles after CNT growth 42

Figure 20: Effect of Cr in multilayered catalyst 44

Figure 21: Ternary phase diagram for Cr-Ni-Fe at 800°C 45

Figure 22: VACNT growth on different substrate using multilayered catalyst 46

Figure 23: Graph of carbon concentration profile of a growth process 50

Figure 24: Effect of growth duration on CNT growth 52

Figure 25: 5 min VACNT growth vs prolonged 30 min growth 55

Figure 26: Graph of carbon concentration profile 56

Figure 27: Local carbon concentration effect 57

Figure 28: Local carbon concentration demonstration 58

List of Abbreviations

Fe	iron
Ni	nickel
Cr	chromium
Si	silicon
Al_2O_3	aluminum oxide
SiO_2	silicon dioxide
Ar	argon
SEM	secondary electron microscopy
TEM	transmission electron microscopy
EDX	energy dispersive x-ray spectroscopy
CNT	carbon nanotube
SWNT	single-walled carbon nanotubes
MWNT	multi-walled carbon nanotubes
VACNT	vertically aligned carbon nanotube
AC	amorphous carbon
NINT	National Institute for Nanotechnology
sccm	standard cubic centimeters per minute

1 Introduction

Nanometer scale technology has advanced into 21st century with tremendous momentum. CPUs now contain 100s of millions of transistors packaged into centimeter-sized dies capable of processing billions of calculations per second. Modern cell phones have MP3, video, and GPS capabilities and are simultaneously light and compact. Computer monitors and TVs are brighter and more vibrant with dimensions of unimaginable 3 mm in thickness. On the advanced material front, the use of metal hydrides [1,2], carbon fibers [3] and polymer materials [4] led to great progress in hydrogen storage, light weight high strength material and pharmaceutical applications respectively. All of these great achievements are the result of our ability to process materials and structures in sub-micron regime. Materials of even smaller dimensions are being actively researched to further reduce device size and cost while improving performance [5,6,7].

Carbon nanotubes (CNTs) have shown great potential in improving existing technologies as well as in enabling new ones. CNTs were officially recognized by Dr. Sumio Iijima in 1991 during an arc discharge experiment to produce C_{60} [8]. Since their discovery, CNTs have attracted significant interest from both academic and commercial sectors [9,10,11]. The intense interest is the result of CNTs' highly ordered nano-sized 1-dimensional structure. Quantum mechanical

phenomena become significant at nanometer dimensions and provide CNTs with their unique properties that are usually superior to conventional materials [12,13,14].

CNT products have not penetrated the market because the growth technology has not matured enough to warrant consistent and controlled high volume production. This bottleneck still exists even after nearly two decades of research. Therefore it is important not only to investigate deeper into the CNT growth mechanism, but also to focus on high volume production aspect of growth. The difficulty with high volume CNT production is that academic research is mostly carried out in small CVD systems that are only capable of processing small pieces of substrate [47]. When such technology is transferred onto a larger CVD system, the previously established growth parameters do not properly address the prolonged temperature ramp up step, increased effect of flow dynamics, the influences of substrate orientation and so forth. Therefore, CNT research using a high-volume-production CVD system directly addresses the technology transfer issue and is able to push CNT technology into commercial success much more rapidly.

The purpose of this project is to establish a vertically-aligned carbon nanotube (VACNT) growth process in a high volume Tystar CVD system situated at the National Institute for Nanotechnology (NINT). This kind of research presents great novelty in studying and optimizing catalyst designs and growth conditions suitable for large CVD systems. Many phenomena are expected to occur that would not otherwise exist in a small CVD system and hence provide insights into the CNT growth mechanism. The Tystar CVD system in NINT uses the state of the art control systems to regulate process temperature and gas flow rates much more consistently as compared to small CVD systems. The experimental results will therefore be more consistent and reliable. And lastly, the direct applicability of technologies established on a high volume CVD towards high volume production further enhances the value of this project.

This chapter will go over the physical characteristics and properties of carbon nanotubes. It will also describe VACNTs and their important toward the advancement of CNT technology. Methods for CNT growth and catalyst preparation are discussed in Chapter 2. Chapter 3 establishes the experimental details of this project. Chapter 4 covers the experimental results that lead to the optimization of a novel multilayered catalyst for VACNT growth. Chapter 5 provides in-depth discussions on the roles each of catalyst materials on the enhancement of VACNT growth, and the significance of preventing amorphous carbon (AC) formation. A gas concentration model and local concentration theory are also established to explain many phenomena that occurred throughout the project, and directions are provided for optimizing the growth recipe to achieve ideal results. Finally, Chapter 6 will touch on the future research directions.

1.1 Physical Characteristics

CNTs are generally categorized into two general types: single-walled carbon nanotube (SWNT) and multi-walled carbon nanotube (MWNT). SWNT can be viewed as a graphene folded into a seamless cylinder. MWNTs consist of multiple layers of these concentric cylindrical shells (Figure 1). SWNTs can have diameters ranging from 0.4 nm to 3 nm [15,16,17]. For diameters smaller than 0.4 nm, a high degree of orbital bending makes the structure energetically unstable. Larger diameter SWNTs are rarely seen because they lack the structural integrity to sustain the cylindrical arrangement [36].The case is rather different for MWNTs. The interspacing between concentric graphitic shells is approximately the same as that of graphite [17]. Interlayer Van der Waals forces provide structural support for the inner layers of a MWNT. Therefore MWNT can have diameters up to 100s of nanometers. The ends of CNTs are capped by hemispherical fullerenes with diameters equaling that of the corresponding CNTs.

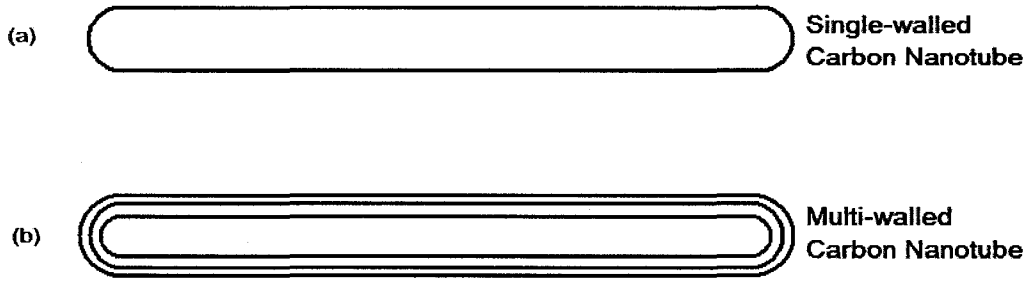

Figure 1: Single-walled and Multi-walled carbon nanotubes

The orientation of the graphite folding with respect to CNT growth direction is called the chirality of the SWNT. Due to the similarity between the CNT shell and graphene, CNT chirality is described by graphene basis vectors $\boldsymbol{a_1}$ and $\boldsymbol{a_2}$. Any hexagon on the graphene sheet can be described by a vector $\boldsymbol{c}$ according to equation,

$$\boldsymbol{c} = n\boldsymbol{a_1} + m\boldsymbol{a_2}$$

where n and m are integers and corresponds to the required steps along the basis vectors to reach a particular hexagon from a point of origin. This vector $\boldsymbol{c}$ is called the chiral vector (Figure 2). If the circumference of a SWNT perpendicular to its length corresponds to a chiral vector $\boldsymbol{c}$ described by a set of n and m indexes, then (n,m) indexes the chirality, or the direction of graphene rolling, of that particular SWNT. The chiral indexes (n,m) also determines the electronic properties of CNT. All SWNTs with (n,m) indexes that satisfy the condition,(n-m)/3 = integer, are metallic. Otherwise, they are semiconducting [22]. The notable cases for metallic CNTs are the armchair with n=m and zigzag with m=0. For MWNT, each shell will have a chirality of its own, but categorizing their electronic properties is much more complicated.

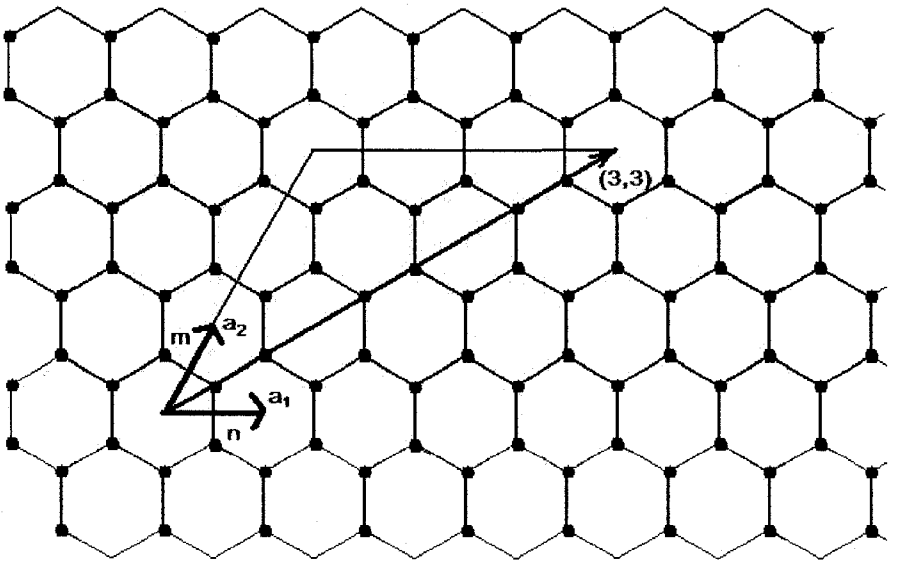

Figure 2: Graphene sheet with (n, m) chiral vectors

1.2 Properties and Applications of CNT

The most interesting and technologically important aspects of CNTs are their material properties. Their highly ordered 1-dimensional structures provide them with novel characteristics not seen elsewhere. The electrical, optical, mechanical and chemical properties of CNTs have all shown potential and in most cases superior performance than many current state-of-the-art technologies have to offer. Many properties of CNT are dependent on their physical dimensions which can be controlled during synthesis [18]. The highly tunable properties of CNT enhance their potential for use as the next generation material in many applications.

1.2.1 Electronic Properties

As mentioned earlier, the electronic properties of CNTs directly depend on their chiralities. The "(n-m)/3 = integer" rule separates the CNTs into two electronic categories of semiconducting and metallic CNTs. Most of the researches focus on electronic properties of

SWNTs due to their smaller dimensions and more pronounced confinement effect, as well as their simpler structure where the properties can be directly derived from the properties of graphene [17,19].

Metallic SWNTs can have low resistance and high current carrying capacity. The perfectly ordered structure of SWNTs in absence of localized surface states provides them with ballistic transport behavior, a phenomenon of electrons go through a conductor without undergoing any scattering events, over micrometer range [20,21]. Metallic SWNTs are also able to carry an extremely high current density of 10^9 A/cm^2 [22]. These characteristics of metallic SWNTs are promising attributes in device interconnects where low resistance and high current capacity is crucial.

The bandgaps of semiconducting SWNTs are inversely proportional to the diameter of the SWNTs. A 1 nm diameter semiconducting SWNT has a bandgap in the range between 0.7 - 0.9 eV [23,24].The conductivity of these SWNTs is closely dependent on the location of the Fermi level. A capacitively coupled gate voltage can move the Fermi level of a semiconducting SWNT into the conduction band to transform the SWNT into a conductor [25,26]. Together with the small dimension of SWNT, these properties makes them promising candidates as electron channels for field effect transistors (CNTFET). Furthermore CNTs can be doped to further modify their conduction behavior [27].

CNTs also have extraordinary field emission performance. When compared with carbon fibers, CNTs' small dimensions greatly improve their field enhancement. Field emissions from CNT have been observed at fields lower than 1 V/μm with high density of 1 A/cm^2 [28,29]. Individual CNTs are excellent emitters, but physical damage during emission leads to reduced emission performance. The fabrication of individual CNT emitter arrays is also extremely difficult.

CNT films and VACNTs also have good emission performance, and thus are more suitable for field emission applications because of ease of fabrication and device reliability [36].

1.2.2 Optical Properties

CNTs have 1-dimensional structures that offer highly ordered optical bands and sub-bands. In addition SWNTs have direct band gaps that make them good light emitters for optoelectronic applications, where optical emission can be obtained in absence of phonon excitation [30,31,32]. Optically excited light emissions from suspended individual CNTs have been experimentally observed [33]. Optical emissions can also be obtained from electrical excitation in FETs [34] and electron injection into MWNTs through STM [35]. The emission wavelength from a semiconducting CNT can theoretically vary from 300 nm to 3000 nm. The wide emission range means CNTs can be used in blue lasers and IR detectors [36]. When the CNTs are in bundles, optimal emissions are rarely observed as the electrons and holes transfer between the neighboring CNTs to undergo non-radiative recombination [29].

CNTs' ordered emission spectra are constantly employed to study the structure of CNTs themselves. Raman Spectroscopy uses the optical absorption from the excitation of vibrational modes in CNTs to determine the diameter of the SWNTs and also the amount of defects in the sample [37]. From the luminescence spectra together with Raman spectra of CNTs, a two-dimensional plot can be created. Chiral indexes (n,m) can be assigned to each of the peaks on the plot, revealing the chirality profile of the CNT sample [30,38] .

1.2.3 Mechanical Properties

The C-C γ bond is the strongest bond in nature. Both experimental measurements and theoretical calculations have shown that CNTs are as stiff as or stiffer than diamonds with the

highest Young's modulus and tensile strength among known materials [39]. The Young's modulus of CNT is independent of the tube chirality but dependent on the tube diameter [40]. Smaller tubes are less mechanically stable while larger tubes have their Young's modulus approach that of graphite. CNTs have a Young's modulus typically on the order of 1 – 2 TPa [39,41], superior to diamond and much higher than those of carbon fiber and steel. MWNTs tend to have higher modulus than SWNTs due to inter-shell Van der Waals forces improving the overall stiffness. The tensile strength of CNTs ranges from 10 GPa to over 100 GPa [42], which is over 10 times greater than those of diamond and carbon fiber. The elastic response of a nanotube to deformation is equally remarkable. Most hard materials fail with a strain of 1% or less due to propagation of dislocations and defects. Both theories and experiments have shown that CNTs can sustain up to 15% tensile strain before fracture [43]. This extraordinary property is credited to the strain release through sp^2 rehybridization. The mechanical properties of CNTs make them ideal for mechanical sensors, composite materials, and to replace carbon fiber in high strength light weight materials.

1.3 Vertically-aligned Carbon Nanotubes

VACNT is a special orientation of CNTs that can be both single-walled and multi-walled. CNTs assert Van der Waals attraction forces to other nearby CNTs [44]. If the CNT density is high enough, the attraction forces from all directions hold CNTs perpendicular to the substrate during and after growth, similar to the electric field lines of a large plate. The condition for VACNT growth is to provide sufficient crowding in order to maintain vertical CNT growth. Single-walled and multi-walled VACNTs are regularly grown in CVDs [45,46,47]. Even though most

applications may not require ultralong CNTs, centimeter long CNT are indicators of a potential of VACNT growth process, and their ability to adapt to applications of all dimensions.

Current CNT growth technology does not provide sufficient control over CNT quality, size, chirality and growth direction [36]. A collection of CNTs provide better performance predictability and manufacturability than with individual CNTs [48]. This is where VACNT is advantageous as they are intrinsically high in density, and adequate performance predictability can be achieved in a relatively small area. Thus, these VACNTs can be used to make electron channels in FETs or act as field emitters in field-emission-displays. The high density and small dimension of VACNTs are ideal for applications that require high surface area to volume ratios such as energy storage and chemical sensing. Moreover as long as the surfaces are oriented properly, the vertical nature of VACNT allows for directional growth without external assistance. CNT bundles offered by VACNTs will not have the same kind of performance sharpness as a single SWNT [39], but VACNT devices are able to overcome the shortcomings of current CNT growth technology that are preventing the commercialization of CNTs. Therefore products incorporating VACNTs are the more realistic commercial opportunities for the near future.

2 Carbon Nanotube Growth Methods

To implement CNTs into actual devices, the CNTs need to be synthesized and selectively placed at localized areas. CNT synthesis, or growth, occurs from the self-assembly of carbon atoms at temperatures higher than 600°C [49]. In fact, CNTs were first recognized as a new type of material during a high temperature process to produce C_{60} [8]. In order to commercialize CNT technology, CNT growth needs to be carried out reliably and reproducibly. Establishing technologies granting precise control on the number of shells, diameter, length, chirality and growth location of the resulting CNTs tailored toward the application of interest is also essential. To grow CNTs, carbon vapor needs to be delivered to the vicinity of growth sites which are maintained at elevated temperatures range from 600°C to over 2000°C. Currently there are three established methods that accomplish the task – arc discharge, laser ablation and chemical vapor deposition.

2.1 Arc discharge

Arc discharge is the first method used to grow CNTs. The setup contains two carbon electrodes situated very close to one another inside a vacuum chamber with small amount of Ar or He flow [50]. A low current, high voltage power supply charges up the electrodes to initiate an arc discharge. The intense energy of the arc discharge sublimates the graphite electrode into

carbon vapor which then condenses onto the other electrode (Figure 3). The arc discharge creates a high temperature environment upwards of 3000°C within the discharge chamber. At such elevated temperature, the sublimated carbon atoms realign themselves into hexagonal structures similar to graphene and form CNTs.

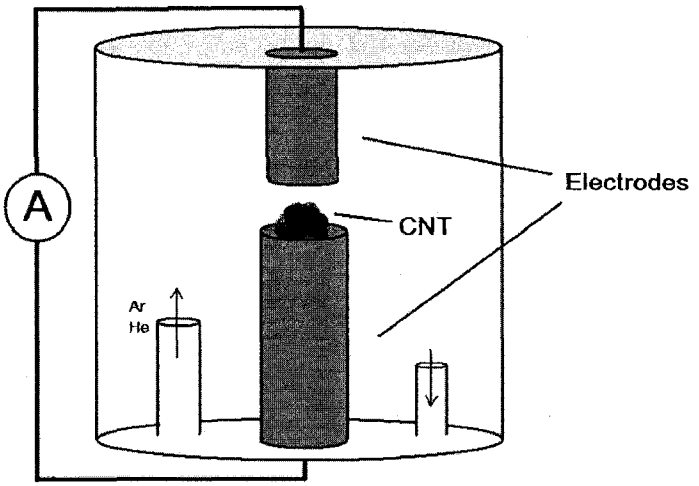

Figure 3: Diagram of an arc discharge setup for CNT growth

Arc discharge can produce MWNTs without assistance from external agents. However, SWNTs require the presence of transition metal catalytic nanoparticles, such as Fe, Ni and Co, to regulate CNT diameters. The metal content is directly incorporated into the graphite anode to be vaporized together the carbon. Arc discharge is carried out at extremely high temperatures. Therefore SWNTs grown by arc discharge are usually low in defects as the carbon atoms have sufficient energy to move about to form hexagonal lattice which is the low energy state [51]. Large amount of CNTs can be grown with arc discharge and several companies are selling arc grown SWNTs commercially.

Arc discharge has several issues. The high temperature environment during growth limits the type of materials that can be placed inside the chamber, and thus makes device integration extremely difficult. Also because of the high process temperature, other variations

of carbon material form just as readily. CNT samples from arc discharge have large quantity of different types of fullerenes and the highly undesirable amorphous carbon (AC). Additionally these grown CNTs are always tangled together in web-like morphology [40]. Therefore, extensive post-process purification and tube-separation steps are required. After purification, arc discharge CNTs need to be transferred, and depending on applications, manually placed onto specific locations. Such placement is a slow and daunting task, and does not lend itself well to high volume parallel integration in areas such as the microelectronic industry.

2.2 Laser ablation

Laser ablation setup involves a quartz tube containing a graphite target. The tube is filled with Ar, He or N_2 to create an inert environment [52]. Heating elements are placed around the quartz tube to maintain a chamber temperature of between 800°C and 1200°C. On one end of the tube is a laser source that is used to heat the graphite target up to 3000°C the sublimate the graphite. On the other end of the tube is a water cooled metal collector tip, usually copper, to condense and collector the CNTs (Figure 4). CNT nucleation occurs in the vapor phase and the temperature gradient established by the heating elements around the quartz tube drives the CNTs towards the cooled collector tip. Similar to arc discharge, SWNTs can be grown in the presence of transition metal nanoparticle catalysts that are embedded into the graphite block [53].

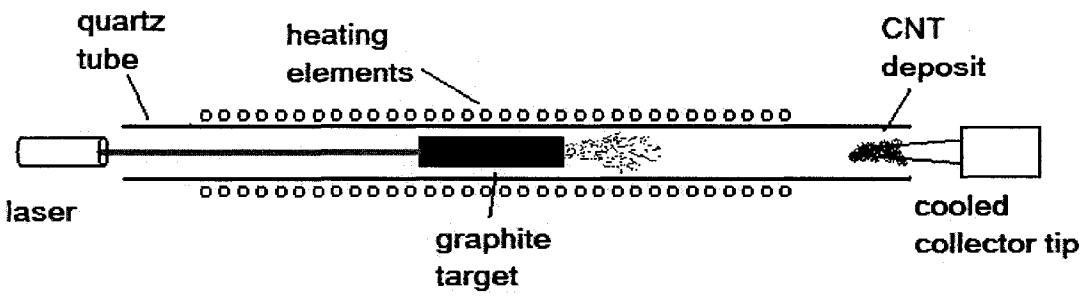

Figure 4: Diagram of a typical laser ablation chamber

Aside from the carbon sublimation method, laser ablation and arc discharge operate at very similar growth conditions and produce CNTs similar in quality as they are both high temperature processes. Laser ablation offers operator greater level of control of the growth parameters than arc discharge through direct manipulation of laser intensity and pulse frequency if the laser is pulsed. Presently, arc discharge and laser ablation are the methods of choice for large-scale CNT production. However laser ablation suffers the drawbacks similar to those of arc discharge. High growth temperature limits material and process integration. CNTs cannot be directly grown onto substrates. Significant amount of impurities such as fullerenes and amorphous carbon are also produced along with CNTs. Laser ablation has the potential to be scaled-up, but the setup including the laser and power consumption is rather expensive. Overall, arc discharge and laser ablation are great technologies to produce high quality CNTs, but the lack of compatibility with process and material integration limits usefulness of these growth methods for applications especially in the electronic and optoelectronic fields.

2.3 Chemical vapor deposition

For CNTs to be widely employed in consumer products, CNTs' physical dimensions need to be precisely controlled. Contaminations of AC, fullerenes and other non-carbon contaminates need to be eliminated. CNTs need to be precisely placed at only the desired locations in a

parallel fashion to reduce production time and cost. Both arc discharge and laser ablation have difficulties satisfying these requirements. On the other hand, chemical vapor deposition can deal with the above mentioned issues in a more controlled manner and is widely recognized by both scientists and industrialists as the only viable method to push CNT devices into the commercial market [36,40]. Therefore it is not surprising that CVD method is currently the most used growth method among researchers [45,47,54].

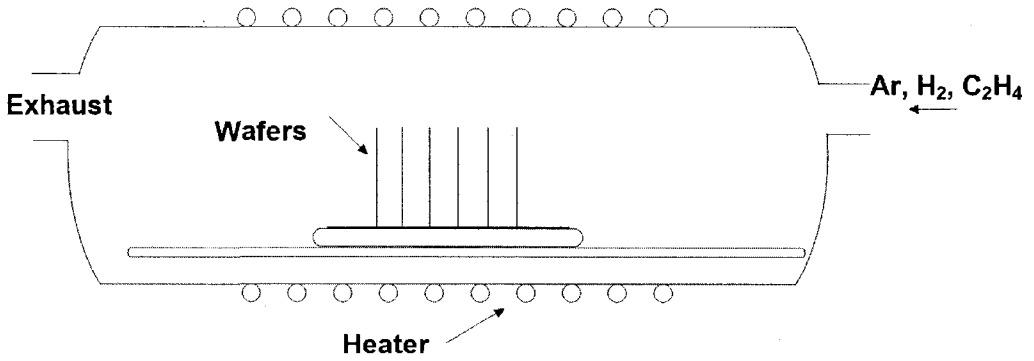

Figure 5: Diagram of a chemical vapor deposition setup

Chemical vapor deposition systems contain a quart tube as the process chamber like in laser ablation. The temperature of the chamber is regulated through the heating elements around the tube. Gas flow controllers are used to deliver carbon containing feedstock gases, such as CH_4, C_2H_4 and CO, directly into the process chamber. Other gases that are also used during CNT growth are Ar and H_2 (Figure 5). CNT growths in CVD are usually carried out at temperatures between 600 and 1000°C, which is much lower than the growth conditions in arc discharge and laser ablation processes. The low process temperature improves CVD CNTs' compatibility towards material and process integration. Fullerene and AC contaminations can be mostly eliminated by optimizing the growth recipe. However, the reduced growth temperature tends to produce CNTs with higher defect density than those from the high temperature

processes as some carbon atoms may not have sufficient energy to align into perfect hexagonal structures [55]. Recent advances in CNT growth technology have virtually eliminated differences in quality between CVD CNTs and arc discharge or laser ablation CNTs. Another crucial advantage that CVD has over the two high temperature methods is its capability to grow CNTs directly onto substrates. Depending on the size of the CVD system, CNTs can be grown on small substrate pieces in home-made CVDs or on multiple full sized substrates in large high volume CVD systems. Therefore, CVD growth technology is capable of high throughput production of both CNTs and CNT-integrated devices. Nevertheless, arc discharge or laser ablation still has a much higher CNT production rate than what the CVD can currently achieve.

CVD requires transition metal nanoparticle catalysts to grow both SWNTs and MWNTs [56]. The catalyst preparation method for CVD growth is entirely different than the method used in arc or laser growth processes. Instead of incorporating the catalyst into the carbon source, the catalysts are deposited onto the substrate before the CNT growth is carried out in a CVD system. There is a very crucial advantage for pre-growth catalyst deposition employed for CVD growth. By patterning the location of the catalysts on the substrate through etching or liftoff, the growth location of CNTs can be precisely controlled and significantly reduces the complexity of incorporating CNTs into devices. These catalytic particles are usually prepared chemically into a solution which is then spun onto the substrate and dried, or physically through sputtering or e-beam evaporation directly onto the substrate. For chemically prepared catalysts, the particles are suspended in a solution [57]. For physically deposited catalysts, as long as the deposition quantity is low, the catalyst atoms gain energy and agglomerate into particles to reduce surface tension at high temperatures [58].

The widely accepted CNT growth mechanism with catalyst is the vapor-liquid-solid(VLS) model [56]. Under the model, carbon feedstock dissociates at the substrate surface, catalyzed

by metal nanoparticles, to release carbon atoms. These carbon atoms get absorbed into the catalytic particles. Once the catalytic particles become supersaturated with carbon atoms, the carbon atoms segregate from the catalyst and arrange into a cap structured like a hemispherical fullerene following the contour of the catalyst. As more carbon atoms are absorbed, they are continuously incorporated into the root of the initial cap to form cylindrical shells (Figure 6). Therefore the diameters of the CNTs are closely associated with the size of the catalytic particles.

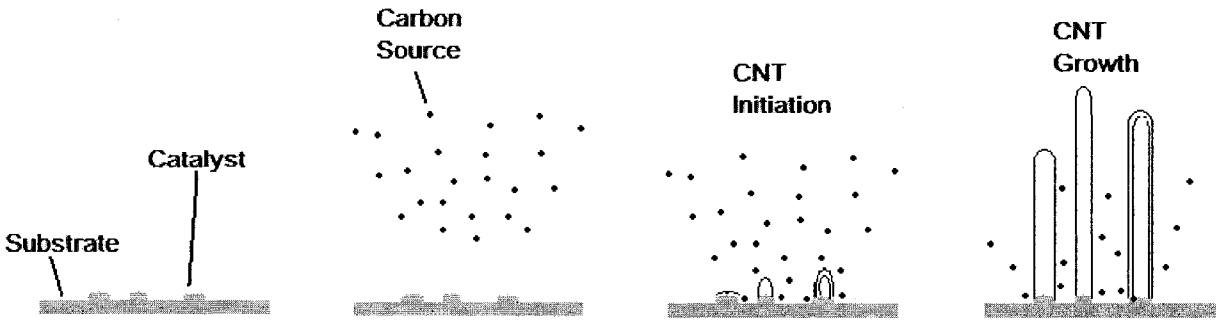

Figure 6: Diagram illustrating VLS growth mechanism

CVD has been used successfully to grow SWNTs, MWNTs and VACNTs with CNT length reaching millimeters long. Many prototype devices such as CNTFET [59], field emitters [28], hydrogen storage medium [60] have been demonstrated due to CVD's ability to grow CNTs onto selective regions of the substrate surface. Regardless of CVD's successes in growing CNTs, the understanding of the exact mechanism behind CNT growth is currently unknown. Theories such as the VLS model can provide insights into the growth process. However there are still critical factors involved in the CNT growth that are unclear to the academic community. Experimental results obtained from one laboratory are likely irreproducible when transferred into another laboratory [61]. This is evident from the literature where a large number of growth conditions and catalyst designs are used by different research groups. Many complex catalysts are established usually because a simpler catalyst design that works in one laboratory would not

work on their equipment. These inconsistencies hinder the process of scaling up CNT growth in CVD, as the technologies established on home-made CVD systems in research laboratories do not transfer into high throughput CVD systems very well. Nonetheless, significant efforts are under way to correct the current technological shortcomings and bring CNT products into commercialization.

2.4 Catalyst Preparation

As previously mentioned, the CVD process requires metallic nanoparticles, such as Fe, Ni or Co, to catalyze CNT formation, and CNT diameters are directly dependent on the catalytic particle sizes. Catalytic CVD processes have long been utilized for growing carbon filaments. The difference between carbon filaments and carbon nanotubes are their dimensions. Carbon filaments are larger in size with diameters over 100nm, while carbon nanotubes usually have diameters much less than 100 nm [40]. Therefore the key to initiate carbon nanotube growth as opposed to carbon filaments is to use catalytic particles of nanometer dimensions.

The two general methods to deposit catalysts are direct deposition through physical vapor deposition (PVD) or spin-on coating for chemically prepared catalysts. Chemically prepared catalysts use structure-direction agents in the base solution to regulate the shape and size of the to-be-synthesized nanoparticle [62]. Metal containing solutions, such as $Fe(NO_3)\cdot 6H_2O$, are then added to the base solution. Chemically prepared catalysts can be made to have very small and uniform diameter nanoparticles [63]. However, this kind of preparation is very time consuming.

On the other hand, there are two deposition methods for PVD: electron-beam (e-beam) evaporation and sputtering. In sputtering, ions bombard a sputter target composed of the material to be deposited. Momentum transfer on the surface of the sputter target due to ion

bombardment ejects atoms from the sputter target towards the substrate for deposition. The sputtering process is highly reproducible and can have high throughput. E-beam evaporation uses electrons to heat up the material inside a graphite or alumina crucible. As the material increases in temperature, its vapor pressure increases accordingly. Film deposition occurs from the ejected material vapor landing onto the substrate [64].

To form nanoparticles, a thin film of catalyst material of a few nanometers or less in thickness is deposited onto the substrate. The substrate containing the catalyst film is then annealed at temperatures between 500°C and 1000°C. At high temperatures, catalyst atoms gain sufficient energy to have mobility on the substrate surface, and agglomerate into particles to reduce surface tension. PVD techniques are very widely used to deposit catalyst materials because of their reliability and ease of use [45,47,65].

3 Growth of Vertically Aligned Carbon Nanotubes

For this project, e-beam evaporation and CVD will be used to grow CNTs. The focus of the project and the methodology are structured to take advantage of the unique high-volume production capabilities available at the University of Alberta and NINT to aid local CNT research and to be a step above as compared to conventional academic CNT research. This chapter will cover the details as well as justifications of the experimental procedures and growth methodology employed in nanoparticle catalyst preparation, CNT growth and post-growth characterization. The experimental results and in depth discussions will be covered in the subsequent chapters.

3.1 Catalyst preparation methodology

Catalysts are prepared by e-beam evaporation. The reasons for using e-beam evaporation are manyfold. In terms of production capability, e-beam evaporation is capable of much higher throughput than chemically synthesized catalysts which require many hours for reactions to complete. Deposition by e-beam evaporation is also simpler and does not leave unwanted residues on the substrate when compared with the chemical synthesis method. Lastly, the uniformity of e-beam evaporation is significantly better than then spin-on and dry process.

Compared with sputtering, evaporation operates at higher temperature and also lacks behind in precision and reproducibility. However, the sputtering systems available locally lack the control and flexibility for short depositions. Sputter rates are usually indirectly calculated from film thickness and deposition length. At the nanometer and sub-nanometer regime, the morphology of the deposited material is likely to be in island formation. Therefore, it is impossible to measure the film thickness or the deposition rate through interferometry or microscopy. Investigating and optimizing CNT growth and catalyst design requires the deposition parameters to be changed frequently. Therefore great difficulties will be encountered if such process is to be carried out by sputtering.

On the other hand, the local e-beam evaporator contains a crystal thickness monitor. A crystal thickness monitor measures the change in vibrational frequency of a crystal due to mass change from the deposition of evaporated material. The values of density and geometric factors are then used to calculate film thickness indirectly from mass. At the nanometer and sub-nanometer regime, the thickness reading from a crystal thickness monitor indicates the amount of material deposited onto the substrate. As such this measurement tool is perfect to monitor nanometer and sub-nanometer depositions.

For this project, catalyst materials are deposited using the Gomez e-beam evaporation system located in Nanofab at University of Alberta. This e-beam evaporator is a single wafer system that contains a manually operated shutter. This manual shutter is used to its advantage to create a catalyst zone profile across the wafer by exposing varying amount of the substrate during deposition (Figure 7).

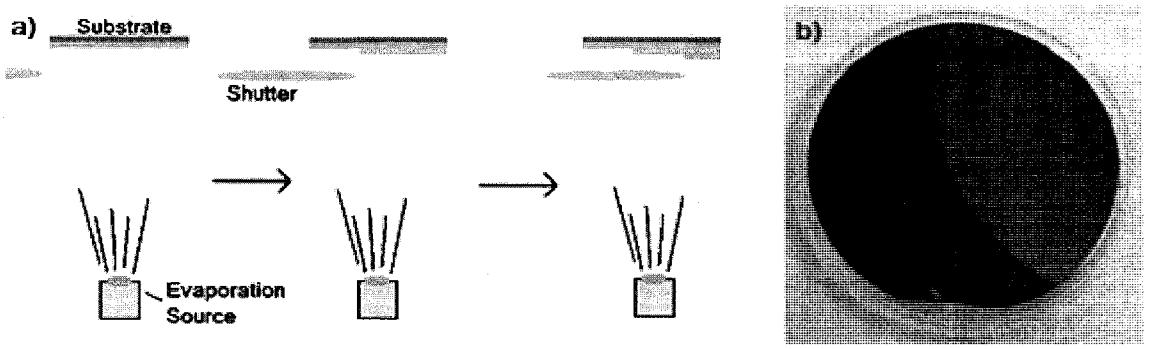

Figure 7: Thickness profile from shutter manipulation

a) Illustration of manual shutter manipulation. b) Substrate with thickness profile after CNT growth

All of the experimental trials, such as for the effect of Fe film thickness on CNT growth, can thus be performed on a single substrate to eliminate any unsuspected variations that may result from separate evaporations. This guarantees that any differences seen between different catalyst zones are strictly due to the effect of catalyst variation on CNT growth, and therefore provides more reliable experimental results when investigating the effects of different catalyst designs.

3.2 CNT growth Setup

CNT growths were carried out in a high volume Tystar atmospheric CVD system. This CVD system is capable of processing up to 50 10" substrates per run. For practicality reasons, only 4" substrates are used. The system also employs state-of-the-art control systems to accurately and consistently regulate process temperature and gas flow rates. The operation commands are programmed into a digital recipe file which the CVD system follows to automatically carry out the process. The entire CVD growth process includes sample loading, temperature ramp up, CNT growth, and cool down. The use of high volume CVD system allows

the established technology to be much more applicable towards commercialization than the conventional laboratory CNT researches, and the advanced control modules enhance the reliability of the experimental results.

3.3 Procedure

First of all, it is generally accepted that pure transition metal catalysts form silicide when in contact with Si at high temperature [66]. Silicide particles are not active catalysts for CNT growth. To separate the catalyst from the Si substrate, a SiO_2 barrier layer is usually used. Forming SiO_2 through wet oxidation is simple and provides great film quality and uniformity.

4" (100) Si substrates are first Piranha-cleaned to remove organic and other surface contaminants. The cleaned Si substrates are then placed into the Tystar CVD furnace, the same one used for CNT growth, for oxidation at 1000°C for 30-60 min. After oxidation, the wafers are examined through interferometry to determine the oxide thicknesses. Oxidations in Tystar furnace have consistently yielded uniformity of < 2% across wafer and < 1% across a 25 wafer load.

Oxidized substrates are then loaded into Gomez depending on the experiment for catalyst deposition. The substrate chamber is pumped down to $1x10^{-6}$ torr before the deposition materials are heated up by the electron gun. The deposition rates are usually maintained at 0.1 nm/s for all materials to improve precision. Fe, Co and Ni have all shown catalytic effect in CNT growth. Many types of elemental and alloy composite catalysts have yielded excellent CNT growth [65]. Nevertheless, Fe and Fe-containing catalysts are by far the most preferred catalyst among researchers and generally provide better growth results [47,71]. For this project, a multilayered catalyst is used. The catalyst design and how each individual material contributes to VACNT growth will be discussed in the later chapters.

Once the catalysts are deposited onto an oxidized substrate, the substrate is placed in the Tystar CVD furnace to perform the CNT growth. The furnace tube idles at 550°C. Once the substrate is placed into the furnace, temperature is ramped up to the desired growth temperature in 45 min. The temperature ramp up step also anneals the deposited catalyst film to form nanoparticles. During the substrate transfer from e-beam evaporator to the CVD, oxygen in air will oxidize the deposited catalyst material. The catalytic capability of the catalysts is greatly reduced in oxidized state [40]. Thus, 100 sccm of H_2 is flowed into the furnace carried by 2400 sccm of Ar during the ramp up to reduce the oxidized catalysts into their elemental form. For the CNT growth step, the carbon feedstock C_2H_4 is carried by Ar. C_2H_4 is used because previous experiments performed by Hata and et al. produced millimeter long single-walled VACNTs [47], something that would be nice to reproduce on Tystar. H_2 is also introduced to the gas mixture. The role of H_2 in CNT growth will be discussed later. Most of the experiments are performed with one substrate per growth. The sample substrate is always placed between two dummy substrates to simulate the gas flow effect of a multi-substrate process. Finally, the furnace is cooled down to between 250°C and 450°C under 3000 sccm Ar, and the substrate is then taken out of the furnace.

Overall the CVD process contains three general steps. The first is the temperature ramp up step. This step also functions as a catalyst pre-growth treatment step where the catalysts are annealed and reduced into particles of elemental form. The second step is the CNT growth step, where carbon feedstock gas is released into the furnace. The last step is the cool down. This thesis focuses on the parameters of the CNT growth step while leaving temperature ramp up and cool down steps unmodified throughout the project. Also for ease of discussion in later sections, the phrase "growth recipe" will specifically refer to the temperature, gas flow rates and duration of the CNT growth step.

SEM and TEM are used to evaluate catalyst preparation and CNT growth in terms of quantity, density and morphology. There are many other important aspects of CNT properties that require attention. However, since the goal of the project is to establish VACNT growth in high volume CVD not tailored to any specific application, the material properties of CNT are of less importance and are hence not included in the evaluation of CNT growth. The results from this project provide a basis for future work and can be further optimized in future researches to suit the application of interest.

4 Catalyst Design

There are large numbers of variables that affect CNT growth. The catalyst composition, the type of carbon feedstock, the growth temperature, pressure, and duration, the cool down rate and post-growth processing all have significant impact on outcome of the growth. However one of the most important variables is the catalyst design. Earlier in Chapter 1, the physical nature of VACNTs is described and its benefits are explained. VACNT devices are able to avoid the issue of limited controllability over CNT growth using current technologies. In order to grow VACNTs, the catalysts need to have high density. The catalysts should also be active, meaning high percentage of available catalysts lead to CNT growth, under growth conditions. The role of the catalyst is to dissociate carbon feedstock and absorb and organize carbon atoms into CNTs. Carbon atoms also form amorphous carbon (AC) at CNT growth temperature. AC formation around a catalyst can stop carbon atoms or carbon feedstock from reaching the catalyst and render the catalyst inactive. Therefore an active catalyst should be able to process carbon feedstock dissociation and quickly absorb carbon atoms into the catalyst to prevent AC formation from excess carbon. This chapter will provide the experimental results and the optimization process for establishing the catalyst design for enhanced VACNT growth.

In order to judge the effectiveness of different catalyst designs, the activity of the catalyst is used as the guideline. In this thesis, "activity of the catalyst" is a qualitative measure of the ability of the catalyst to process carbon feedstock and control AC formation. The height of

VACNT film is a good quantitative indicator of the catalyst's activity. Thicker VACNT films suggest that the catalysts are able to process the carbon feedstock faster, and hence reduce the amount of carbon available for AC formation and the catalysts can remain in the active state longer.

Researchers have identified several methods to improve the performance of a catalyst design. One is the use of alloys of a catalytic element with a non-catalytic element. A simulation study finds that alloy catalyst particles have significantly increased reaction rate, which may be due to increased reaction sites [67]. Another method to improve catalyst performance is to incorporate Al_2O_3 into the catalyst. Al_2O_3 is a material that catalyzes hydrocarbon reforming, as such may help with the carbon feedstock dissociation process [68]. Even though catalyst-on-SiO_2 have produced good CNTs, there are reports showing undesirable effect of Fe-SiO_2 interaction, such as oxide dissociation [69], which may then form silicides with Fe. The addition of Al_2O_3 separates the catalyst from SiO_2 to prevent catalyst-SiO_2 interaction.

4.1 Controlling catalyst size

The VLS theory described earlier correlates the CNT diameter with that of the catalyst particle. The diameters of carbon nanotubes range from 0.4 nm – 3 nm for SWNT and more for MWNT, therefore the size of the catalytic particles should be nanometer in size. In fact, the sole difference between carbon filament growth and CNT growth is the smaller diameter of CNTs which requires small diameter nanoparticle catalysts.

The catalysts are deposited through e-beam evaporation and annealed. The anneal step transfers thermal energy into the catalyst material, such as Fe. The energetic atoms move around their immediate area and coalesce with other atoms, forming nanoparticles to reduce surface tension. The more atoms there are on the surface, the larger the particles are. Therefore the amount of deposited catalyst or the film thickness of the catalyst layer should be expected

to modify the sizes of the particles. Also the higher the annealing temperature, the more energetic the catalyst atoms become. The longer the anneal lasts, the more time the particles or atoms have to move around. In these cases, the particles are more likely to further coalesce into larger particles. Therefore the anneal temperature and duration will also affect the particle size. In this project, the anneal step is the temperature ramp up step before the CNT growth. The temperature of the anneal varies with time from 550°C to the growth temperature of between 750°C and 850°C over 45 min duration. Thus the temperature and duration of the anneal process cannot be directly controlled, and the film thickness is the variable that can be easily manipulated.

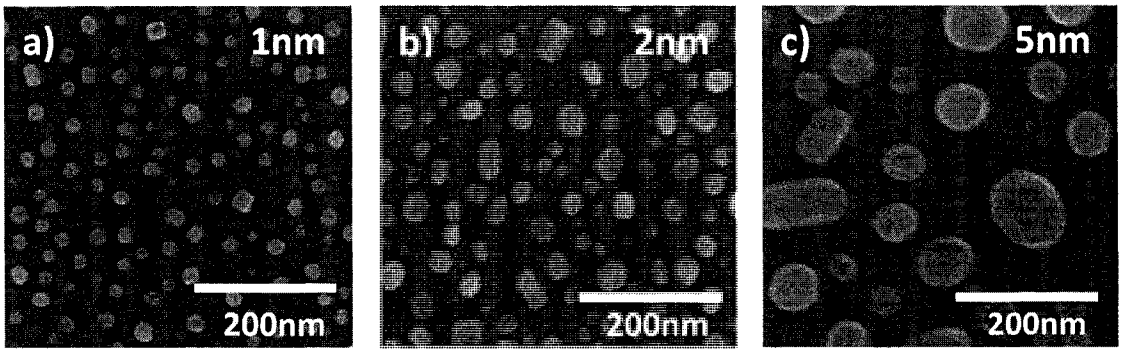

Figure 8: SEM images of annealed Fe nanoparticles

Annealed at 750°C for 30 min, particle on SiO_2 a) 1 nm Fe film, b) 2 nm Fe film, c) 5 nm Fe film

1 nm, 2 nm and 5 nm Fe films are deposited onto an oxidized Si substrate. The substrate is annealed at 750°C for 30 min (Figure 8). There is a very noticeable increase in particle sizes for the 2 nm Fe film relative to the 1 nm Fe film. Annealed 5 nm Fe film shows a significant size increase for the resultant particles. The correlation observed between the catalyst film thickness and the particle size agree with expectation. It is worthy to point out that the particle size for

the 1 nm Fe sample is fairly uniform, whereas the particle size distributions are much larger for the 2 nm and 5 nm sample (Figure 9).

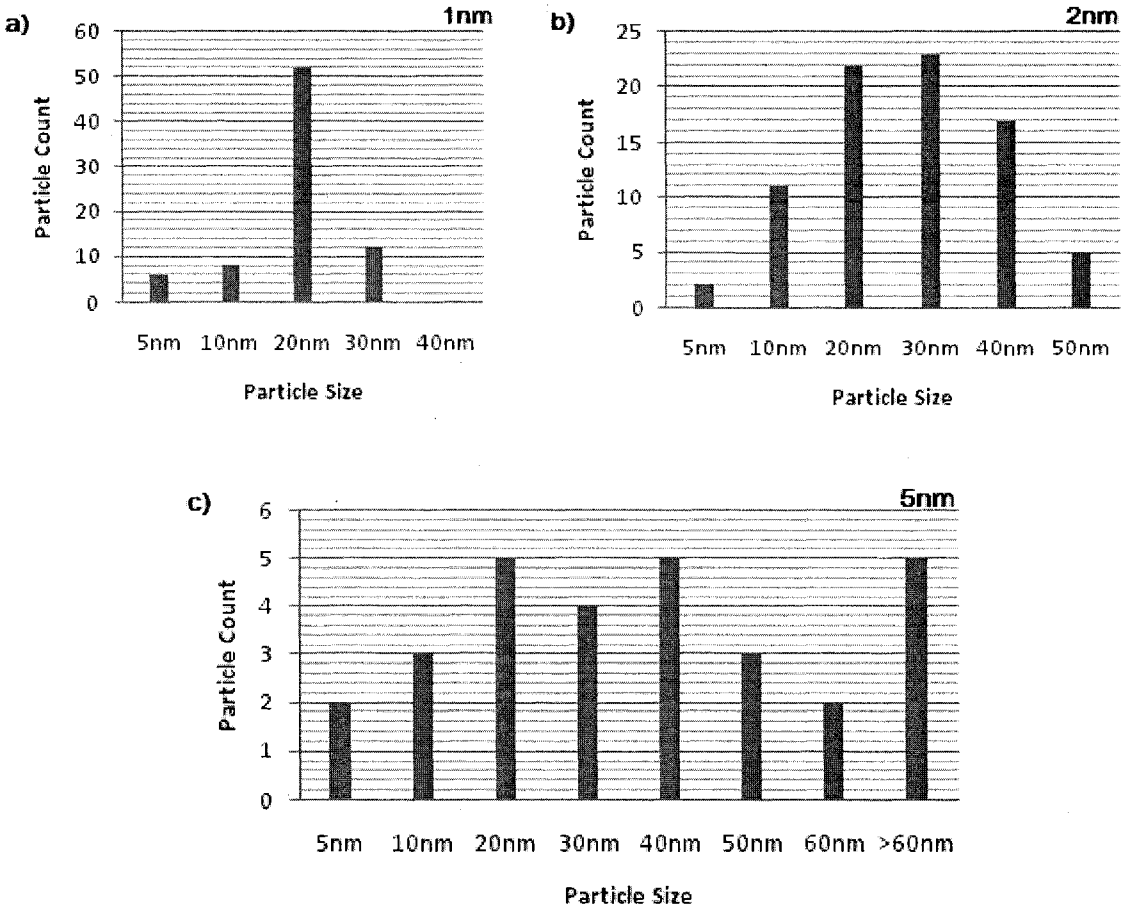

Figure 9: Particle distribution of annealed Fe

The values are hand counted from 0.5 μm x 0.5 μm areas. a) 1 nm Fe film, b) 2 nm Fe film, c) 5 nm Fe film

This is understandable as the more material there is on the surface, the greater the density of particles. Then there are more ways that the smaller particles can coalesce into bigger particles, and hence widen the particle size distribution. Based on the above observation, in order to have small diameter and uniform particles, the amount of catalyst deposition should certainly not be greater than 1 nm of thickness.

4.2 Catalyst composition

This thesis establishes a multilayered catalyst consisting of e-beam evaporated Al_2O_3, Cr, Ni and Fe (this catalyst material combination will be called "the Catalyst" for the rest of the thesis) in their respective order on SiO_2 for growing VACNTs. CNT growth is carried out at 750°C for 5 min with the flow rates for Ar, H_2 and C_2H_4 set at 2500 sccm, 300 sccm and 500 sccm respectively (this growth recipe will be called "the Recipe" for the rest of the thesis). There have been publications that used portions of this catalyst such as Al_2O_3, Cr and Fe, or Fe, Ni and Cr, but there are no publications using this particular catalyst. This catalyst involves more kinds of materials than typical catalyst designs used in other publications. Nevertheless, each of the material in this multilayered catalyst has functions of its own and they work together to enhance the catalytic activity of the catalyst as a whole.

4.2.1 Catalyst Material

Since both Fe and Ni can be used as catalyst on their own, the question is whether the VACNT growth is initiated by Fe or Ni or their combinations. Individually, Al_2O_3 and Cr have shown evidence of their beneficial interaction with catalyst materials to improve activity, but does including both of them into the catalyst, which already contains 2 catalytic materials, improves catalytic activity too? In order to verify whether all of the materials in the Catalyst are playing a beneficial role or is there redundancy in the catalyst design, a combinatorial study of the materials in the Catalyst on CNT is performed.

For 1-element catalyst, two samples are prepared on 400 nm SiO_2 substrates. One sample has 1 nm of e-beam evaporated Fe as catalyst and the other has Ni sputtered at 25 W for 1 min. CNT are grown using the Recipe (Figure 10).

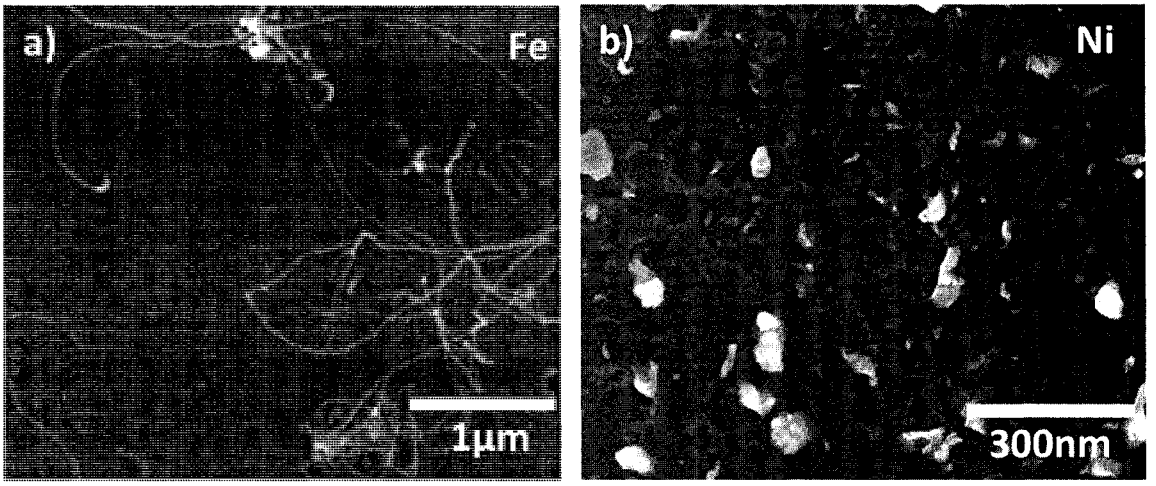

Figure 10: CNT growth from individual Fe and Ni catalysts

a) Fe catalyst, b) Ni catalyst.

The Fe catalyst produces scarce CNT growth. For those grown CNTs, they are microns in length laying on the surface of the substrate. The dark spots on the surface on Figure 10a are the locations of Fe catalyst. Majority of the catalytic particles are inactive and do not produce CNT growth. For the Ni sample Figure 10b, there is no CNT growth anywhere on the substrate. Ni particles are clearly visible surrounded by deposits that are most likely amorphous carbon. Individually, Fe and Ni catalysts do not produce active CNT growth, let alone VACNT growth.

To examine the effect of Fe-Ni alloy and Cr, Ni-Fe and Cr-Ni-Fe catalysts are evaporated on the substrate using manual shutter manipulation to improve the reliability of the result. The thicknesses of Cr, Ni and Fe are 2 nm, 1 nm and 1 nm respectively and the growth is carried out using the Recipe. SEM images of the samples are shown in Figure 10.

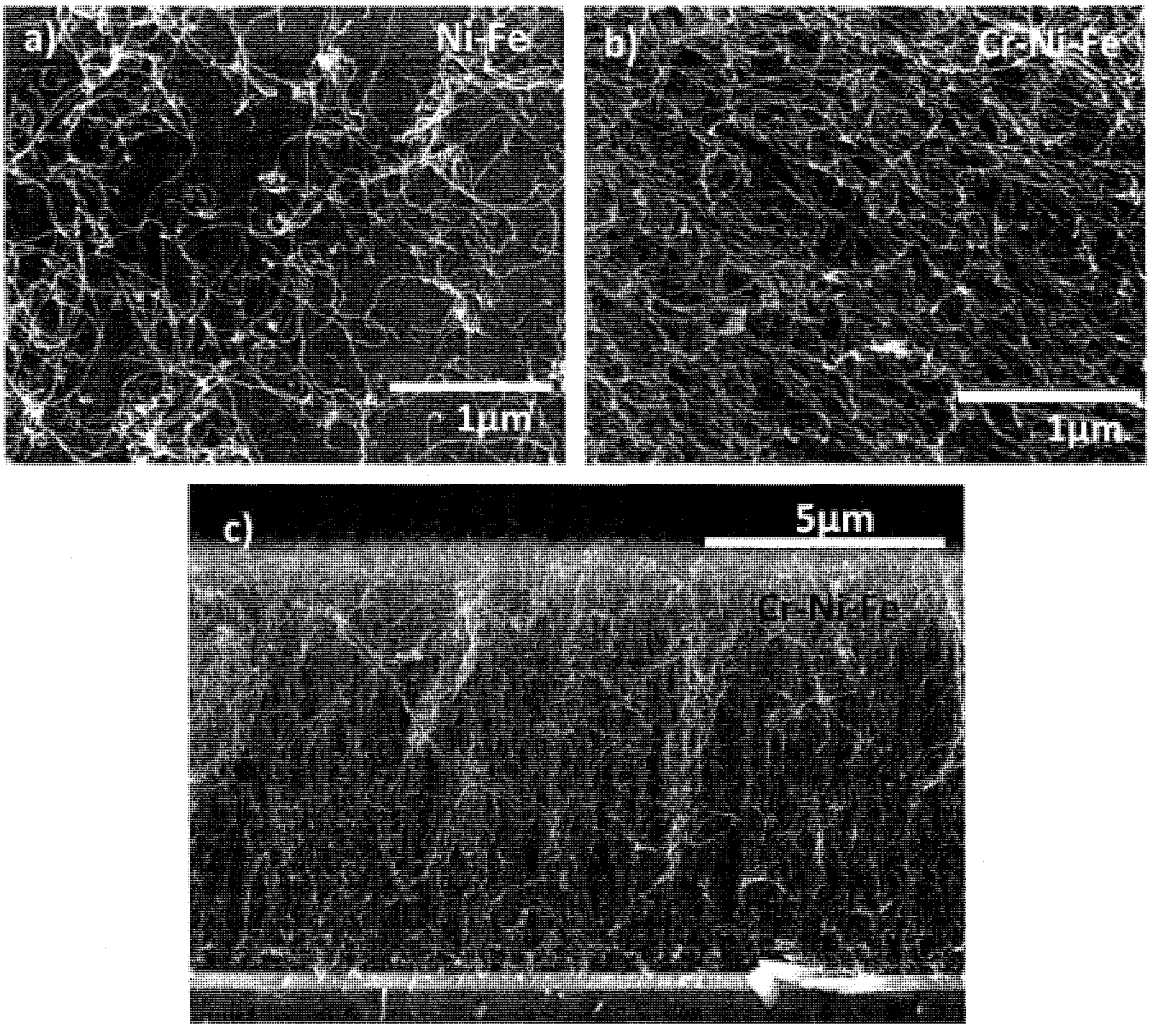

Figure 11: CNT growth from Ni-Fe and Cr-Ni-Fe catalysts

a) Ni-Fe catalyst, b) Cr-Ni-Fe SEM top view, c) Cr-Ni-Fe SEM cross-section view

The Ni-Fe catalyst in Figure 11a produced CNTs in higher density compared with the result from Fe-only catalyst in Figure 10a. CNT growth from the Cr-Ni-Fe catalyst is vastly different than the previously mentioned samples. Looking down from above the sample in SEM (Figure 11b), large quantities of CNTs are grown which completely cover up the substrate surface. From the vertical view (Figure 11c), the CNTs grow vertically away from the substrate to form 12 μm of VACNT. There is small amount of lateral movement for the CNTs during growth, but the general growth direction is vertical. The bright strip between the VACNTs and Si is SiO_2.

Large quantity of VACNT growth with the FeNiCr catalyst shows that the lack of CNT growth on the Fe and FeNi catalyst is not the result of lack of carbon vapor availability at the vicinity of the substrate surface, but the catalyst quality itself. The addition of Ni and Cr onto Fe greatly improves the performance of the catalyst.

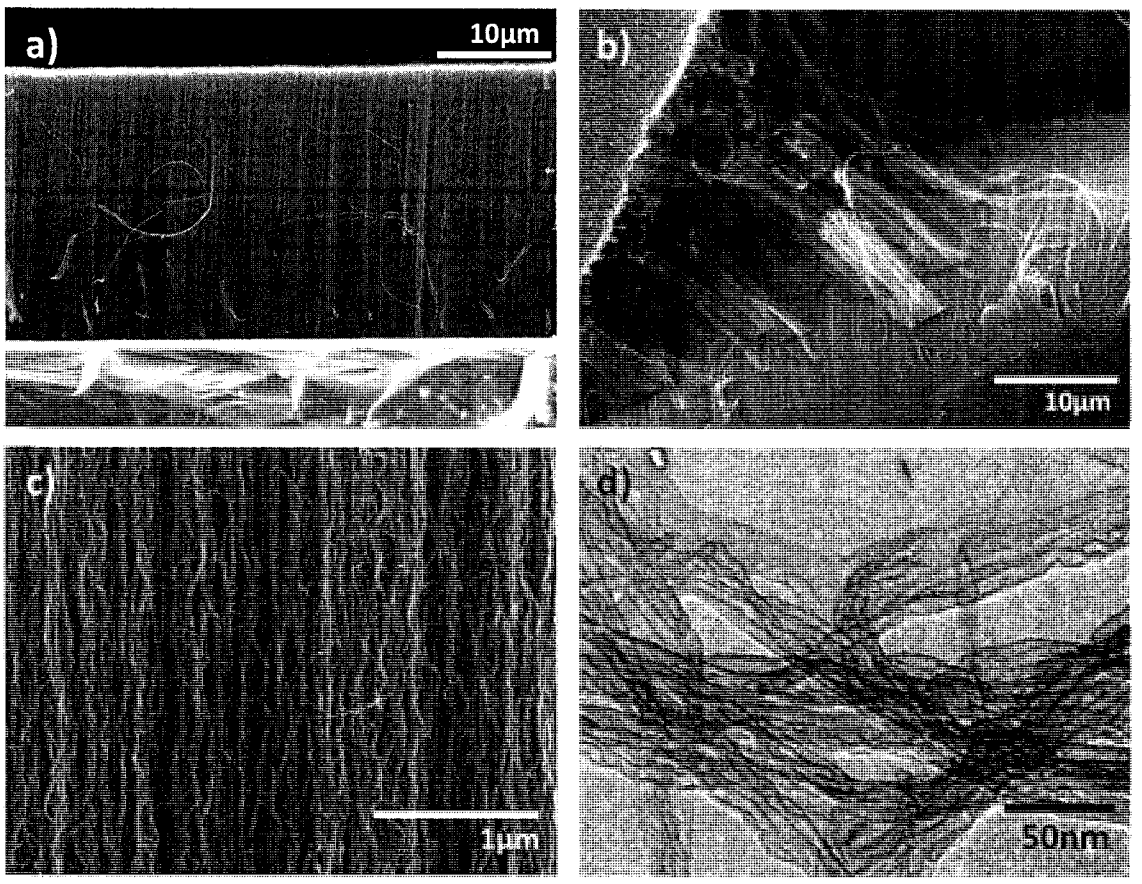

Figure 12: CNT growth from Al_2O_3-Cr-Ni-Fe catalyst

a) and c) SEM cross-section view, b) SEM top down view, d) TEM image

Finally Al_2O_3 is introduced into the catalyst design. The sample contains catalyst composed of 5 nm Al_2O_3, 0.5 nm Cr, 0.5 nm Ni and 0.5 nm Fe (Figure 12). From the Figure 12a and 12c, Al_2O_3-Cr-Ni-Fe catalyst grown with the Recipe leads to VACNT that is much higher in density than results from catalysts without Al_2O_3. The height of the VACNT is also much greater

at 30 μm. As a consequence of the increased CNT density, individual CNTs have much reduced side movements compared with the result from Cr-Ni-Fe catalyst (Figure 12c). The CNTs are also highly entangled. When CNTs peel off from a larger body of VACNT, these CNTs tend to grab nearby CNTs and peel off in the form of threads (Figure 12b). The local uniformity of the growth is very good forming a VACNT film with very flat top surface. From the TEM image of Figure 12d, the diameters of the CNTs are around 5 nm with very thin sidewalls. SWNTs are usually less than 2 nm in diameter, so these CNTs are not SWNTs. During live TEM scanning, these CNTs are clearly seen to be double-walled. However, the TEM operator is unable to obtain a clear still image. Even without a HRTEM image showing the number of walls of the CNTs, it is fairly safe to assume that these CNTs are either double-walled or triple-walled from the 5 nm diameter.

Overall, Al_2O_3-Cr-Ni-Fe catalyst has shown much improved CNT results than other catalyst combinations experimented. The high CNT density is an indication of high CNT yield from the catalysts. The thicker VACNT film compared with that obtained from Fe-Ni-Cr catalyst, signify the catalyst's enhanced processing rate of carbon atoms leading to longer VACNTs for the same growth time.

4.3.2 Optimization of the Catalyst

The Al_2O_3-Cr-Ni-Fe catalyst has shown much improved CNT results than other catalyst combinations experimented, yielding dense long VACNTs. In order to realize the full potential of this multi-layered catalyst, the relative ratio of each material in the catalyst needs to be optimized. Within the catalyst, Fe and Ni are direct catalytic elements that initiate CNT growth. Cr is a supporting element that, according to journal publications, alloy with catalytic element to enhance the catalytic activity of the overall catalyst [65]. Al_2O_3 acts as an underlayer support that separates the catalyst from Si and shapes catalysts and may assist feedstock dissociation

leading to enhanced growth results. The optimization process will be performed on the catalytic portion of the catalyst first, namely the Cr-Ni-Fe catalyst. Then underlayer Al_2O_3 is added to the mix and the layer thickness is optimized to give the highest VACNT with the already optimized Cr-Ni-Fe catalyst. CNT growth conditions will be maintained constant throughout the optimization experiments using only the Recipe.

Cr

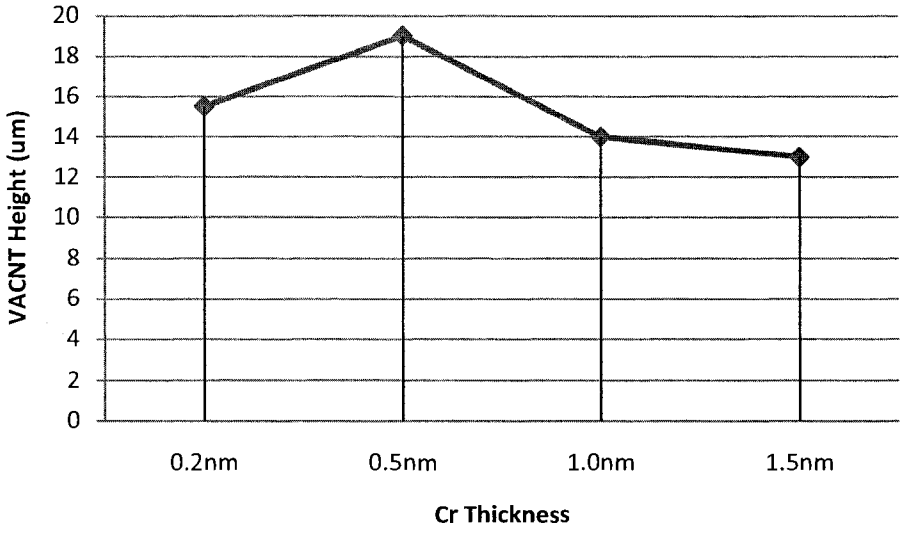

Figure 13: Graph of VACNT heights grown from varying Cr thicknesses

The catalyst also contains 2 nm Fe and 1 nm Ni

Using the manual shutter manipulation, a profile of Cr thicknesses 0.2 nm, 0.5 nm, 1 nm and 1.5 nm is first evaporated onto the substrate. Then 2 nm of Fe and 1 nm of Ni are evaporated on top of the Cr film. The growth results are summarized in Figure 13. The effect of different Cr thickness on the VACNT growth is not significant. The VACNT height gradually increases as the Cr thickness decreases and tops off at 0.5 nm Cr with 19 μm of VACNT. As the Cr

thickness is reduced to 0.2 nm, the VACNT height drops to 15 μm. Hence, 0.5 nm Cr will be used for optimization of Fe and Ni.

Ni

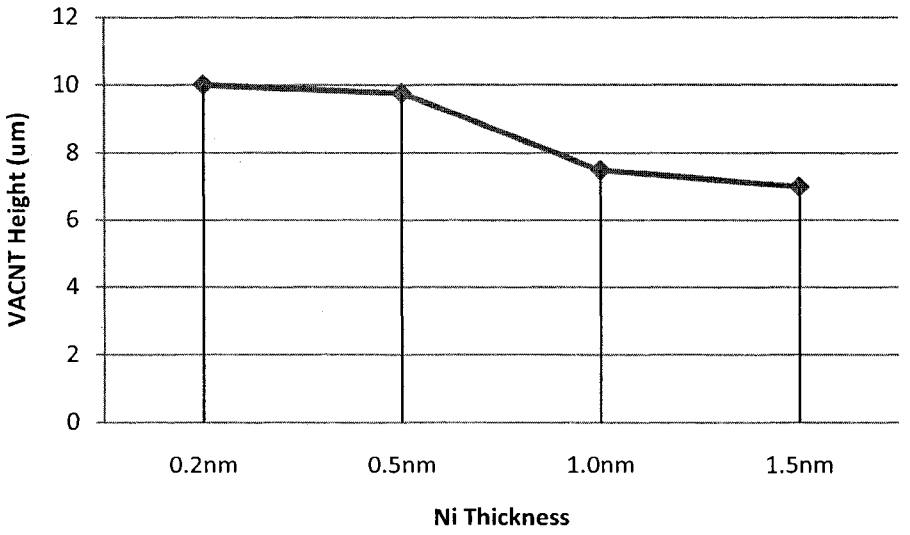

Figure 14: Graph of VACNT height grown from varying Ni thickneses

The catalyst also contains 1 nm Fe and 0.5 nm Cr

Similarly to Cr, manual shutter manipulation is used to create a Ni thickness profile of 0.2 nm, 0.5 nm, 1 nm and 1.5 nm on top of 0.5 nm Cr and below 2 nm Fe (Figure 14). Best VACNT growth is achieved with the 0.2 nm and 0.5 nm Ni regions leading to 10 μm of VACNT. The difference between results from 0.2 nm and 0.5 nm Ni region is not significant enough to argue for the better performance of one thickness as opposed to the other. Therefore 0.5 nm Ni is temporarily chosen as the Ni thickness parameter for Fe optimization. The maximum VACNT height from the Ni experiment is much less than that obtained from the Cr experiment. There are several possible causes of this inconsistency. The crystal thickness monitor's 0.1 nm precision leaves room for noticeable uncertainty for sub-nanometer depositions. It is also

possible that the CVD system has reproducibility issue. However the growth recipe used between the Ni and Cr optimization experiments is the same and all steps of CNT growth are electronically managed by the computer on the CVD. Therefore, it is difficult to point out a step that contains statistical variance that may lead to noticeable reproducibility issue. Furthermore, the CVD furnace is not cleaned between the two experiments, and there is carbon build up on the surfaces of the furnace. The Ni experiment performed after the Cr experiment will have more carbon build up and may have created more absorption sites to further carbon build up. Thus the carbon concentration in the furnace is reduced which will lead to VACNT growth of reduced height.

Fe

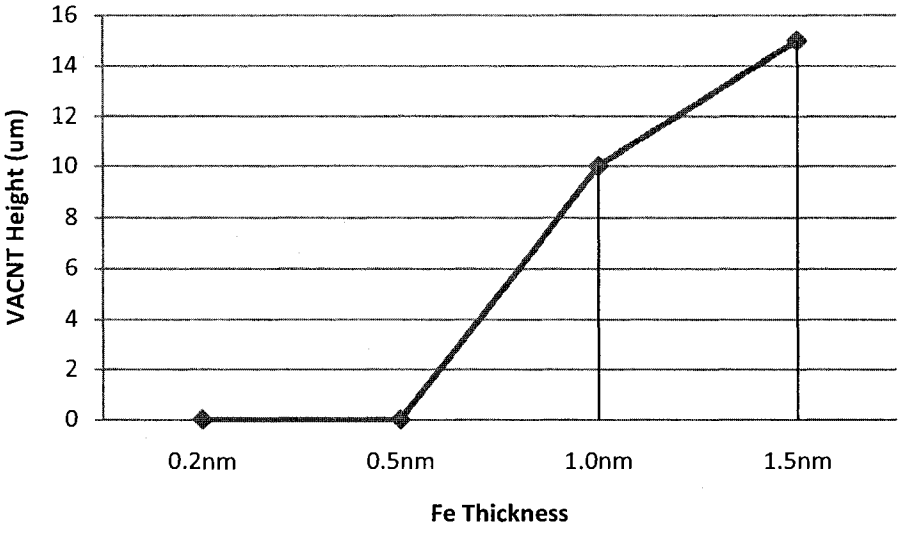

Figure 15: Graph of VACNT height grown from varying Fe thicknesses

The catalyst also contains 0.5 nm Ni and 0.5 nm Cr

With the Fe experiment, Ni and Cr are both at 0.5 nm in thicknesses. Fe thickness profile contains 4 regions: 0.2 nm, 0.5 nm, 1 nm and 1.5 nm (Figure 15). Whereas Ni and Cr offer

noticeable but insignificant growth performance difference from varying film thicknesses, CNT growth has considerable dependency on the amount Fe present in the catalyst. At low Fe thicknesses of 0.2 nm and 0.5 nm, there is only scarce amount of CNTs growth from small number of catalysts. A 10 μm VACNT is produced by 1 nm Fe and 17 μm VACNT by 1.5 nm Fe. It is evident now that higher Fe content in the catalyst helps to improve the activeness of the catalyst. On the contrary, the lower Ni content the catalyst has, the better the CNT growth is, as long as there is Ni present. For this experiment with 0.2 nm of Ni, 0.5 nm of Fe does not lead to VACNT growth. During a later experiment with 0.1 nm Ni and 0.5 nm Fe in the catalyst, VACNT is produced. This indicates that high Fe:Ni ratio is essential for an active catalyst. However it is impossible to deposit sub-0.1 nm Ni with precision and consistency, because the crystal thickness monitor has a display resolution of 0.1 nm. Therefore the Ni thickness of 0.1nm is used as the parameter in the optimized catalyst, even though smaller Ni content may further improve catalyst performance. CNT diameter is directly related to the catalyst size. Higher Fe thicknesses will undoubtedly increase the catalyst size and thus the CNT diameter. In order to maintain small diameter CNT growth, there needs to be a balance between catalyst activity and CNT diameter. With these considerations in mind, 0.5 nm of Fe is chosen as the parameter of choice for later experiments.

Al_2O_3

Al_2O_3 is expected to assist feedstock dissociation and also acts as a separation layer between catalyst and SiO_2. Thicker layers are expected to offer better performance by providing complete catalyst separation from SiO_2. The sample contains a thickness profile of 1 nm, 2 nm, 5 nm, 10 nm, 20 nm and 30 nm of Al_2O_3 films. Fe and Cr are deposited at 0.5 nm in thickness each, while Ni is at 0.2 nm in thickness (Figure 16).

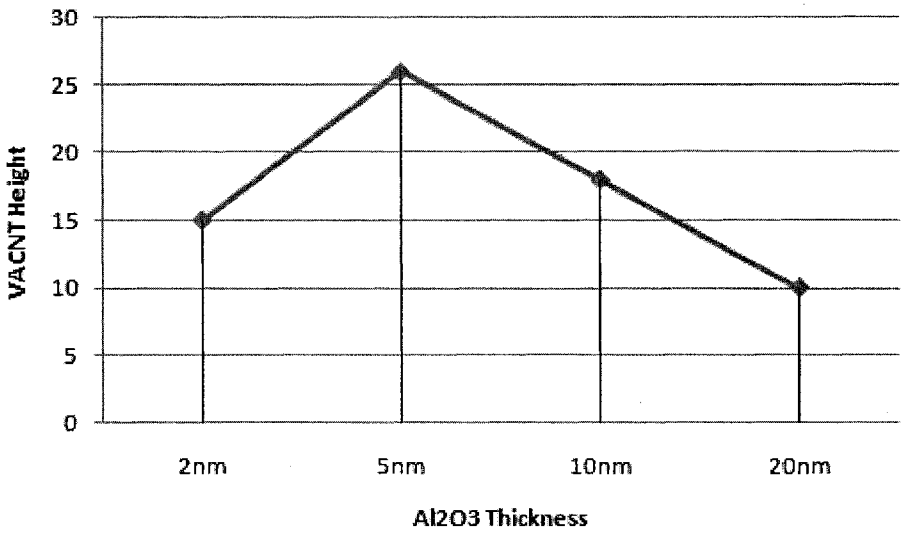

Figure 16: Graph of VACNT height grown from varying Al2O3 thicknesses

The catalyst also contains 0.5 nm Fe, 0.2 nm Ni and 0.5 nm Cr

Interestingly, 5 nm Al_2O_3 region gives the best VACNT growth of 26 μm in height. The poorer results for the thicker Al_2O_3 layers suggest that the proposed separation mechanism does not have significant effect on the growth. Maybe the catalyst still requires some degree of interaction with the SiO_2 underlayer to have the best VACNT growth. The exact reason behind the Al_2O_3 growth enhancement is not known. Further study with SiO_2 underlayer may provide insight into the role of the oxide underlayers for CNT growth.

In conclusion, the semi-optimized catalyst is composed of 5 nm Al_2O_3, 0.5 nm Cr, 0.1 nm Ni and 0.5 nm Fe deposited onto SiO_2 substrates in the order shown in the Figure 17a. The highest VACNT growth achieved with 5 min growth step is 160 μm (Figure 17b).

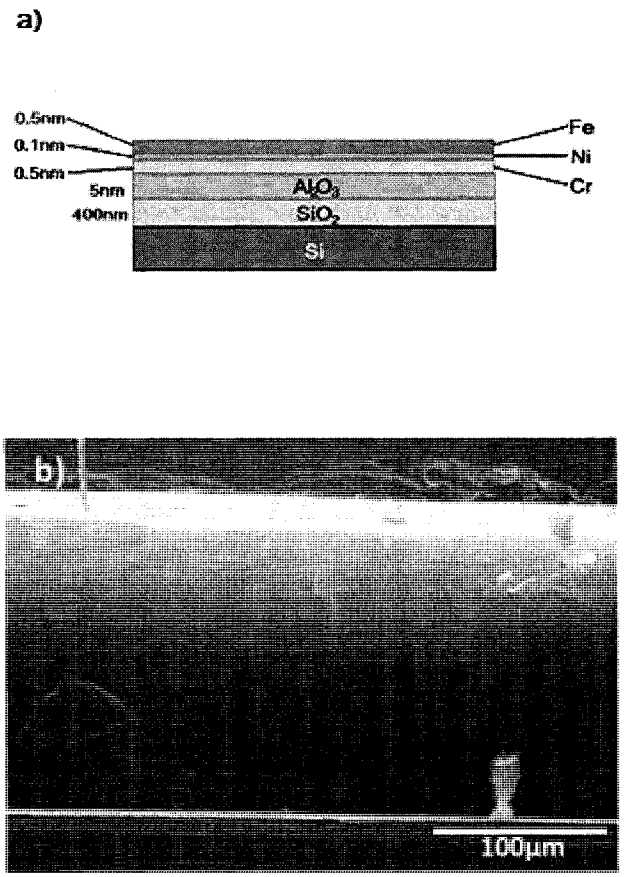

Figure 17: Multilayered catalyst design and consequent VACNT growth

a) Catalyst design, b) SEM vertical view of a 160 µm thick VACNT film

5 Discussion

The ideal catalyst for VACNT growth established in this thesis included variety of elements, and the AC formation was found to be the significant determining factor on the quality of VACNT growth. This chapter will discuss the roles of the materials in the catalyst. A gas concentration model is also established to gain insight into AC formation and how to control the growth recipe to avoid AC, as well as to explain some very interesting experimental results associated with AC formation.

5.1 Effects of individual material in the catalyst

The previous chapter has shown that each of the material in the multilayered catalyst plays a role in enhancing catalytic activity of the catalyst. The amount of Fe in the catalyst has the greatest effect on CNT growth. This implies that Fe is the main catalytic element in the catalyst. High Fe:Ni thickness ratio favors more active catalyst and faster VACNT growth, while Cr and Al_2O_3 act as support materials. Al_2O_3 have long been used in decomposition of hydrocarbons [70]. One theory proposes that Al_2O_3 enhances CNT growth by assisting in the carbon feedstock dissociation [71]. It has been observed that incorporation of Al_2O_3 into the catalyst tends to form smaller nanoparticles [72]. The effect of Al_2O_3 will not be discussed here,

since the explanations given in publications are credible and experiments in this project have not yielded any insights into the role of Al_2O_3. What about the roles of Ni and Cr?

5.1.1 Ni

Fe and Ni form alloy of different phases depending on the relative concentration and temperature. Many literatures have employed alloy catalysts to enhance CNT growth. However, rarely has any reasons been given to explain the function of the alloy.

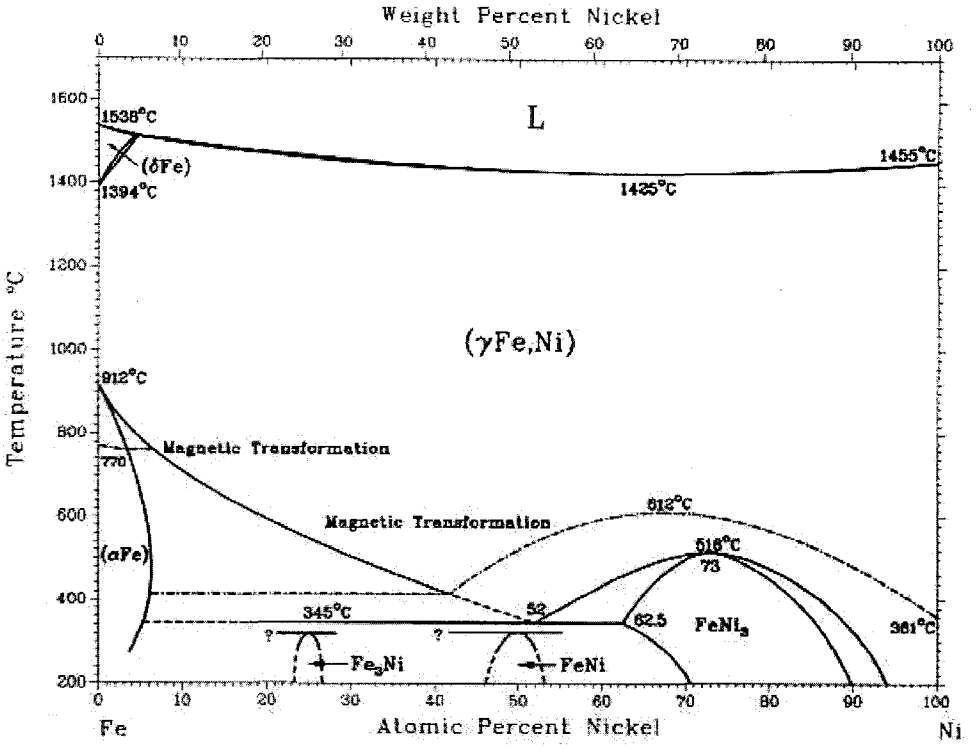

Figure 18: Phase diagrams of Fe-Ni [73]

From the Fe-Ni phase diagram of Figure 18, Fe-Ni alloy at 750°C with Ni atomic concentration higher than 15% is in the γ(Fe, Ni) phase called taenite. Taenite has a FCC structure. With Ni concentration lower than 7%, α(Fe,Ni) phase forms which is a BCC structure

called kamanite. When Ni concentration is between 7% and 15%, a mixture of α and γ phase exist with higher proportion of α phase at lower Ni concentration. From the experimental data and the Fe-Ni phase diagram, the α phase with the BCC structure, forms at low Ni concentration, may have better carbon uptake capability which leads to better CNT growth as judged by VACNT height.

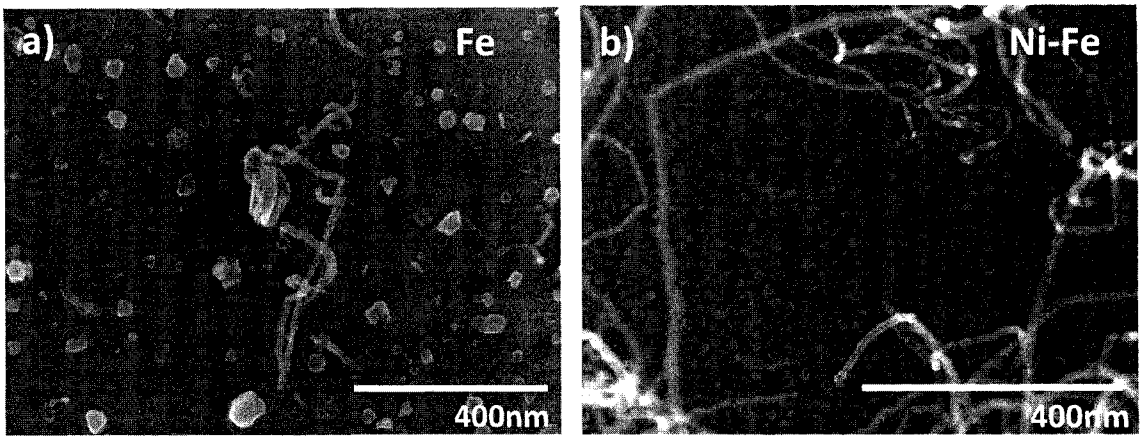

Figure 19: Fe and Ni-Fe catalytic particles after CNT growth

a) 2 nm Fe catalyst, b) Ni-Fe catalyst: 1 nm Fe + 1 nm Ni

Beside the material science, SEM is used to look at the catalytic particles after CNT growth. From Figure 19a and 19b, the particle size distribution of a 2 nm Fe catalyst after 5 min CNT growth at 750°C is much greater than that of a 1 nm-Fe 1 nm-Ni multilayer catalyst after the same growth process. The 2 nm Fe catalyst after growth contains particle sizes range from 10 nm to over 100 nm in diameter. The Ni-Fe catalyst sizes mostly are in range of 20-30 nm. The relatively uniform catalyst size for Ni-Fe catalyst should provide improved consistency across the substrate and also between runs. The improved catalyst uniformity may also contribute to improved CNT growth. Furthermore, the particle density for Ni-Fe catalyst is much higher than that of Fe catalyst. Thus there is more CNT growth sites available leading to higher CNT density.

The increase catalyst density will also decrease the local carbon concentration in the immediate vicinity of the catalyst due to increase carbon uptake rate. How this may affect CNT growth will be discussed in a later section.

5.1.2 Cr

Fe nanoparticles formed at different Cr thicknesses, and TEM energy-dispersive X-ray spectroscopy (EDX) is used to look at the composition of the catalyst after CNT growth. Cr is e-beam evaporated onto SiO_2 surface at 0.2 nm, 0.5 nm and 1 nm in thickness. 1 nm Fe and 1 nm Ni are then evaporated onto the Cr layer. The sample undergoes an anneal step equivalent to the temperature ramp up step of CNT growth process from 550°C-750°C 45 min.

From Figure 20a-c, the catalytic particles have similar sizes of around 20 nm in diameter regardless of the Cr thickness. The nanoparticles of 0.2 nm Cr sample from Figure 20a are very distinct. They are less distinct at higher Cr thickness with deposits filling the gaps between nanoparticles (Figure 20b and 20c). This indicates that Cr may not be incorporated into the nanoparticles, but instead forms an underlayer carrying the Ni-Fe catalytic nanoparticles. This theory explains why nanoparticle sizes do not change with Cr thickness variation. A TEM image of catalytic particle trapped in a CNT grown from Cr-Ni-Fe catalyst on SiO_2 substrate is shown in Figure 20d. The EDX spectrum of that catalytic particle in Figure 20e shows strong signals for Fe and Ni, but Cr is absent from the catalyst; the Cu signal comes from Cu TEM grid used to carry the CNT sample.

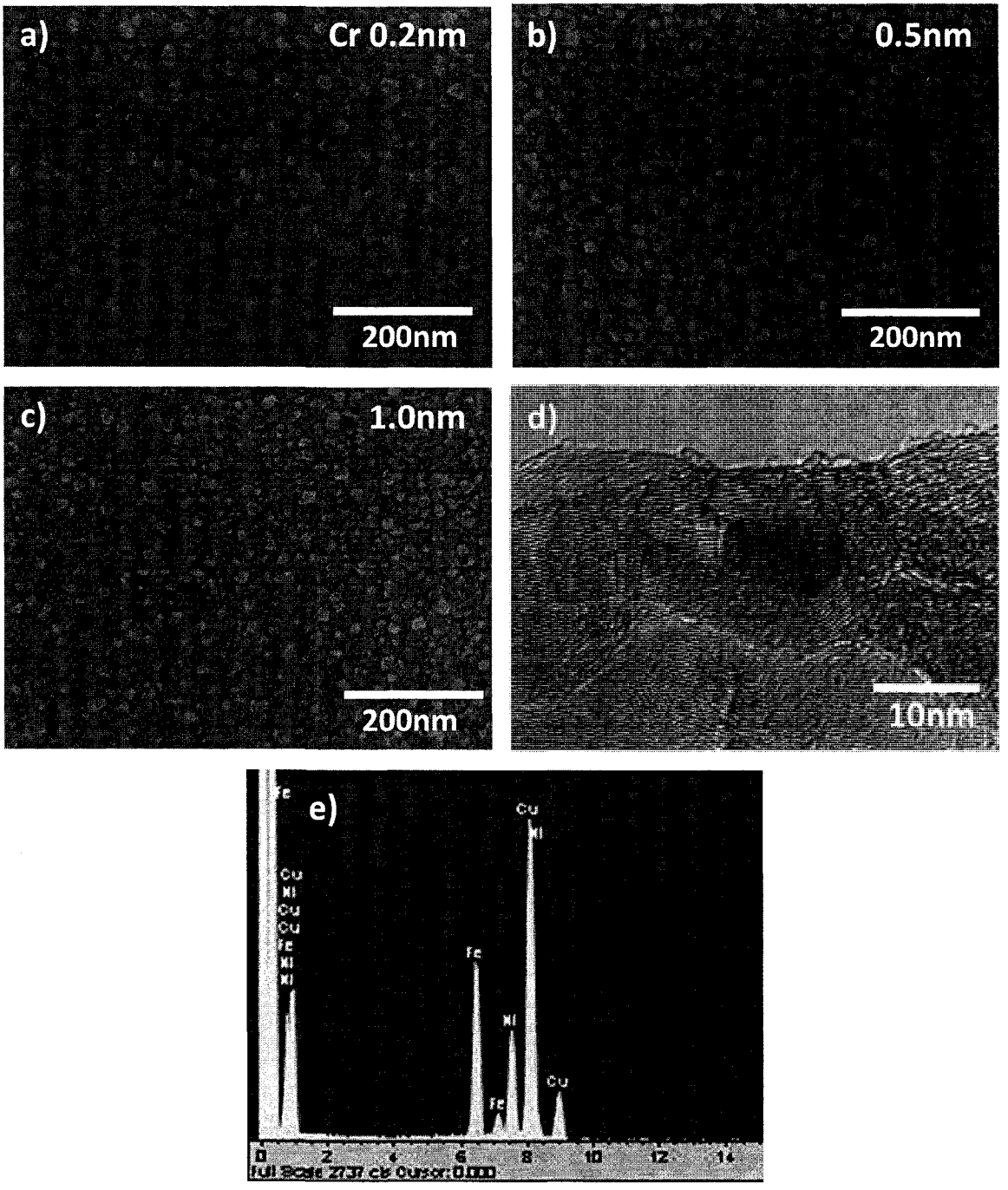

Figure 20: Effect of Cr in multilayered catalyst

a) b) c) shows the effect of Cr on catalytic particle size after anneal, the catalyst also contains 0.5 nm Fe and 0.5 nm Ni. d) TEM image of a catalytic particle wrapped in a CNT. e) EDX spectrum of the catalytic particle in d).

In order to gain insights into the role of Cr in the catalyst, SEM is used to study the Cr-Ni-

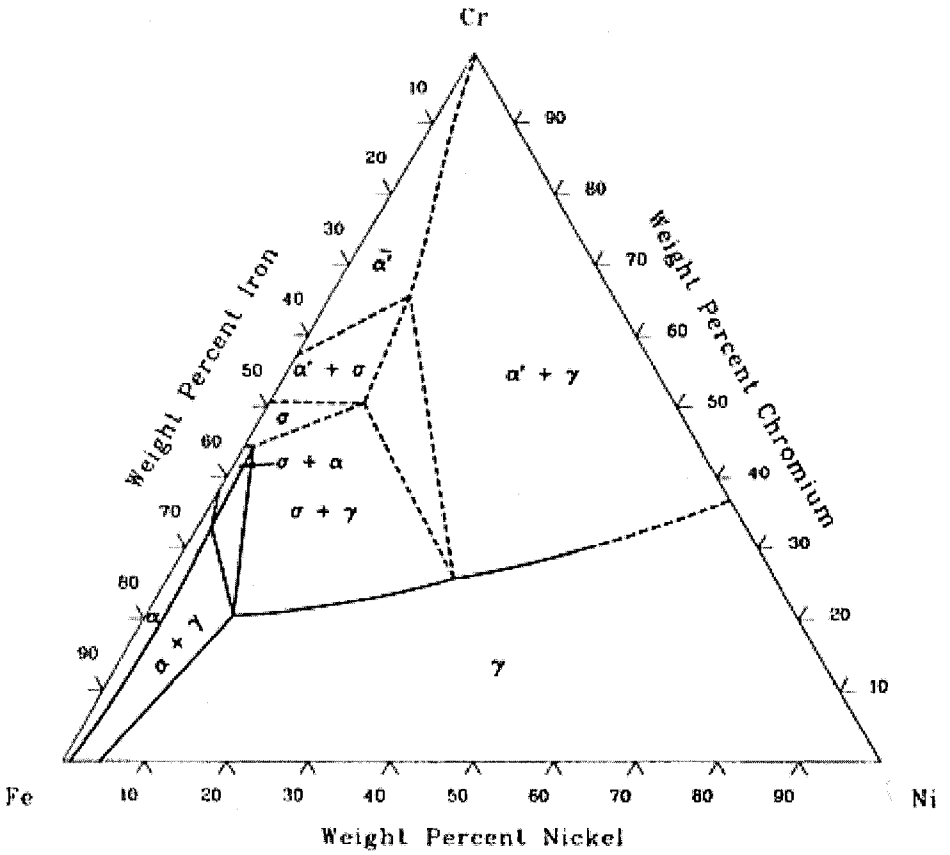

Note: α = (αFe,Cr); γ = (γFe,Ni)

Figure 21: Ternary phase diagram for Cr-Ni-Fe at 800°C [73]

Furthermore from Figure 21, at 800°C Fe and Ni are in the γFeNi phase while Cr is in a separate phase by itself in mixture with γFeNi. All of the evidence show that Cr is not incorporated into the FeNi alloy. Therefore, Cr may help VACNT growth by limiting particle agglomeration during growth to maintain smaller catalytic particle size. However, the exact growth mechanism behind the use of Cr is unknown. A material study of FeNiCr nanoparticle alloy may provide insight into the understanding of catalyst for CNT growth.

5.2 Growth on different substrates

CNT growth is usually carried out on SiO_2 surfaces. SiO_2 acts as a separation layer between the catalyst and Si to prevent silicide formation. In the multilayered catalyst design performed in this project, the 5 nm of Al_2O_3 provide great enhancement to the catalytic activity of the catalyst, and it may also serve as a separation layer.

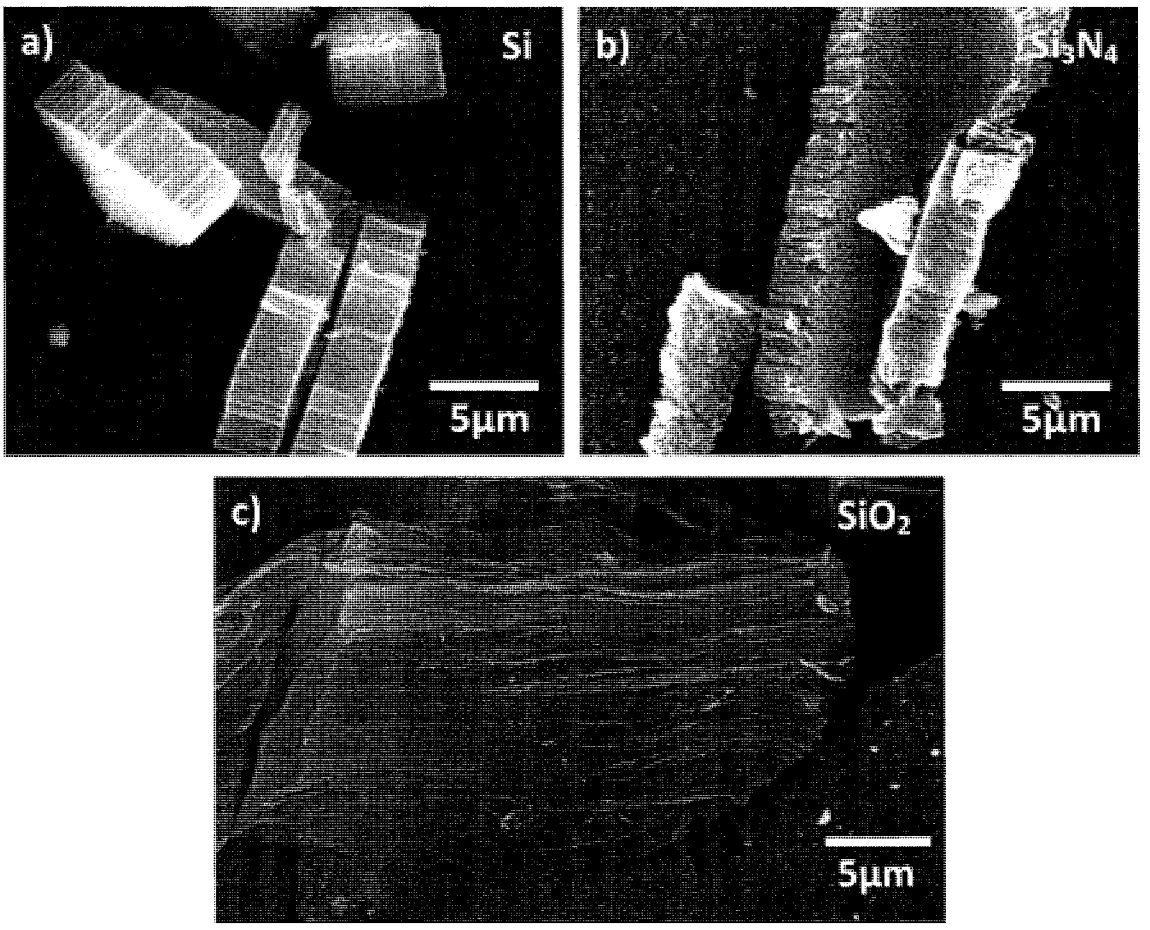

Figure 22: VACNT growth on different substrate using multilayered catalyst

Catalyst used is 5 nm Al_2O_3, 0.5 nm Cr, 0.1 nm Ni and 0.5 nm Fe. SEM top views a) on Si substrate, b) Si_3N_4, c) SiO_2

Thus CNT growths are attempted on three different types of substrates with the multilayered catalyst and the results are shown on Figure 22. On the SiO_2 substrate, a thick film of VACNT is grown as expected with the multilayered catalyst, while only scarce amount of CNT are grown with Fe-only catalyst (Figure 10a). Fe-only catalyst on Si substrate does not produce any carbon nanotubes, while the multilayered catalyst produces 3 μm of VACNT. Similar VACNT growth is also observed on the Si_3N_4 with multilayered catalyst. In conclusion, VACNT growth using the multilayered catalyst is less substrate dependent than the Fe-only catalyst. Finally, the SiO_2 substrate produces much higher VACNT film then the two other substrates. This implies that SiO_2 may still play a role in CNT growth even when used with the already complex multilayer catalyst.

5.3 Gas concentration effect on CNT growth

Catalysts provide the platform for CNT formation, but a suitable growth recipe is required to bring out the full potential of the catalyst. The flow controller on the Tystar CVD system has a maximum flow rate of 5000 sccm. The process chamber has a volume of 40 L. Therefore, it takes roughly 8min or more at full flow rate to entirely fill the process chamber. A growth recipe of 2500 sccm Ar, 300 sccm H_2 and 500 sccm C_2H_4 like that used for most of the experiments for this project, does not mean the gas concentration ratio in the growth chamber is at exactly 25:3 for Ar:H_2 or 5:1 for Ar:C_2H_4 for the duration of the growth process. The furnace is filled entirely with Ar and small amount of H_2 during temperature ramp up. Thus the relative concentration of C_2H_4 in the furnace at the beginning of the growth step when C_2H_4 just started to flow into the furnace is very low. Then the C_2H_4 concentration slowly ramps up towards an equilibrium level as the growth process proceeds. To gain better understanding of the growth process, it is imperative to know how much of each gas is in the process chamber at any given

time. The relative concentration of carbon atoms or carbon feedstock is the most important value to look at, as they are the sources of CNT growth and also AC formation. In the VLS theory, catalytic nanoparticles dissociate carbon feedstock into carbon atoms. During the experiments using Tystar CVD and ethylene feedstock, the surface of the furnace contains carbon deposit after CNT growth. This suggests that ethylene undergoes certain degree of pyrolysis at 750°C growth temperature. The degree of pyrolysis is uncertain. For the sake of establishing a simple model, the catalysts are assumed to only process the carbon atoms from pyrolysis of ethylene. Even though catalysts are likely to process both the carbon atoms and ethylene, the assumption of only carbon atoms interacting with catalysts eliminates one variable from the model. The degree of pyrolysis is dependent on the temperature - the higher the temperature, the higher the degree of pyrolysis, as the atoms have more energy to break the bonds, leading to higher carbon atom concentration. The rate of catalyst-assisted dissociation of ethylene into carbon atoms is also expected to increase with temperature. So the net effect is an increase in carbon concentration seen by the catalyst as temperature increases. In the model, by only counting the carbon atoms from pyrolysis, the increase in carbon concentration from the increased rate of pyrolysis as temperature increases predicts the same qualitative pattern as if the model includes both carbon atoms and ethylene, albeit the actual concentration is different. This qualitative analysis is sufficient for the purpose of gaining insights into the growth process in Tystar CVD. Two more simplifications are employed: the amount of carbon consumed by the catalyst is negligible compared with the amount of carbon atoms that exist in the furnace; and gases diffuse and reach equilibrium instantly in the furnace so that at any moment the concentrations of gases are uniform throughout the process chamber. Before the CNT growth step and the release of H_2 and C_2H_4 gases, the process chamber contains 100% Ar and the relative concentration of carbon C_C is 0. The number of gas molecules in the process chamber, N, is

dependent on the parameters of the chamber, namely temperature T, pressure P and volume V. From ideal gas law,

$$N = \frac{PV}{kT}$$

T remains constant during the CNT growth process. The Tystar reactor is an atmospheric CVD, so P is constant. And V also remains constant. Therefore N is constant throughout the growth. C_C is the ratio of the number of carbon atoms and the number of gas atoms in the furnace, N. Then the change in C_C is,

$$Change\ in\ C_c = \frac{Change\ in\ the\ number\ of\ carbon\ atoms\ in\ the\ furnace}{N}$$

The change in number of carbons in the is equal to the difference between the number of carbon atoms that go into the furnace and the number of those that go out of the furnace. Let C_{in} be the relative concentration of carbon atoms among the input gases, which is a function of the flow rate of C_2H_4 and temperature, or $C_{in} = f(R_{C2H4}, T)$. And let the total gas flow rate to be R. Then the input rate of carbon is $C_{in}RP/kT$ and exhaust rate is C_cRP/kT.

$$dC_c = \frac{(C_{in} - C_c)\frac{RP}{kT}dt}{N}$$

$$\frac{dC_c}{dt} + C_c\frac{R}{V} - C_{in}\frac{R}{V} = 0$$

$K = R/V$ is constant.

$$C_c(t) = C_{in}(1 - e^{-Kt}), \quad t = 0 \ldots t_{cutoff}$$

$$C_c(t) = C_c(t_{cutoff})e^{-Kt}, \quad t = t_{cutoff} \ldots \infty$$

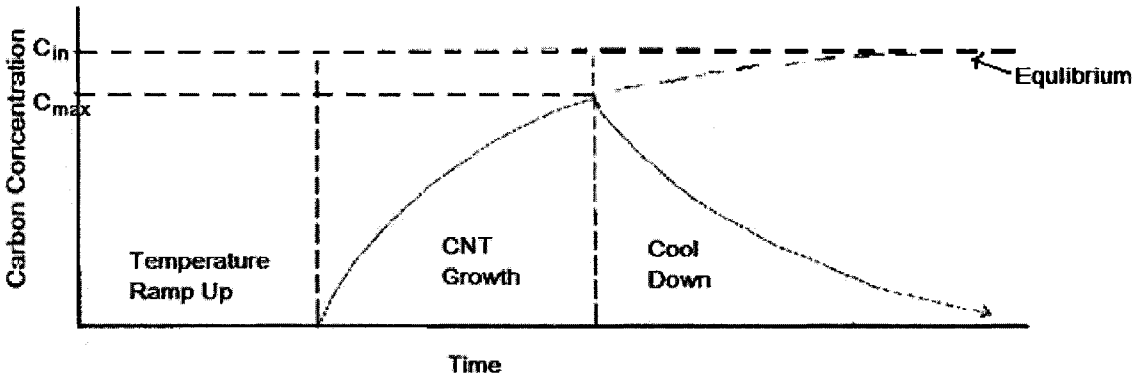

Figure 23: Graph of carbon concentration profile of a growth process

In general an increase in growth temperature and carbon feedstock flow rate leads to an increase in C_{in} and consequently the slope of the ramp up curve for $C_c(t)$.

When carbon feedstock is released into the CVD, CNTs as well as AC form simultaneously. Thus in order to grow CNTs of respectable length, the rate of CNT formation (K_{CNT}) should be maximized, while the rate of AC formation (K_{AC}) should be minimized. K_{CNT} should be dependent on the catalyst characteristics such as the material and the size of the catalyst. Therefore, the ability of the catalyst to absorb C atoms and organize them into tubular shape will put a ceiling on the highest possible K_{CNT} (K_{CNTmax}) for a given catalyst system. Another factor that should affect K_{CNT} is the carbon atom availability surrounding the catalysts. At low C_c, K_{CNT} is limited by the supply rate of carbon, as the catalysts are able to process carbon atoms faster than carbon can replenish. If C_c is increased in this situation, K_{CNT} should also increase up to a point where K_{CNT} reaches K_{CNTmax}. Consequently, any further increase in C_c will not affect K_{CNT}. Of course K_{CNTmax} is directly influenced by the state of the catalyst. As the state of the catalyst changes during growth, K_{CNTmax} will also vary throughout the growth period.

As mentioned above, AC formation occurs along with CNT growth. It is logical to expect K_{AC} to be proportional to C_c. To grow good quality CNTs, the ratio K_{CNT}:K_{AC} should be maximized. At high C_c, K_{CNT} is saturated at K_{CNTmax}, while K_{AC} is still able to increase. Therefore, C_c should be

kept below a level so that $K_{CNT} < K_{CNTmax}$. Low C_c should minimize AC formation and CNT growth can be sustain for longer duration before AC formation poisons the catalysts. Overall, it is reasonable to expect C_c to be the main factor affecting CNT growth. The parameters that effect C_c is temperature, the relative carbon feedstock flow rate and the duration of feedstock release.

5.4 Regulation of amorphous carbon formation

From the gas concentration graph, the level of carbon concentration in the furnace is highly dependent on the duration of carbon feedstock release or the duration of the growth step. At the same flow rate, a 2 min growth step will bring the carbon concentration to a higher level than a 1 min growth step. The increased carbon concentration will increase the undesirable AC formation rate. The effect of growth length to amorphous carbon formation can be clearly seen from the following experiment.

The catalyst used here is 1 nm of e-beam evaporated Fe on SiO_2. The experiments are carried out under the flow rates of 2000 sccm Ar, 100 sccm H_2 and 500 sccm C_2H_4 at 850°C. Three runs are performed with growth time of 7 min, 4 min and 1 min. Figure 24a shows the SEM image of the result from 7 min of growth. The solid base layer on top of the substrate and below the fibrous material is the AC. AC formation fills up the bottom 500 nm of the sample. A closer look at the broken end of the fibers (Figure 24b) reveals another fibrous material with much smaller diameter. This smaller fiber is in fact a CNT buried inside a thick layer of AC. A TEM image Figure 24e shows the inner structure of a CNT covered by AC. The inner CNT with shells are clearly visible from the fringes in the TEM image. The outer portion of the fiber is AC which does not show any ordered structure under TEM. So with this sample, CNTs are initially grown before AC poisons the catalysts. Once the catalysts are poisoned, CNT growth stops whereas AC continuously form on the grown CNTs.

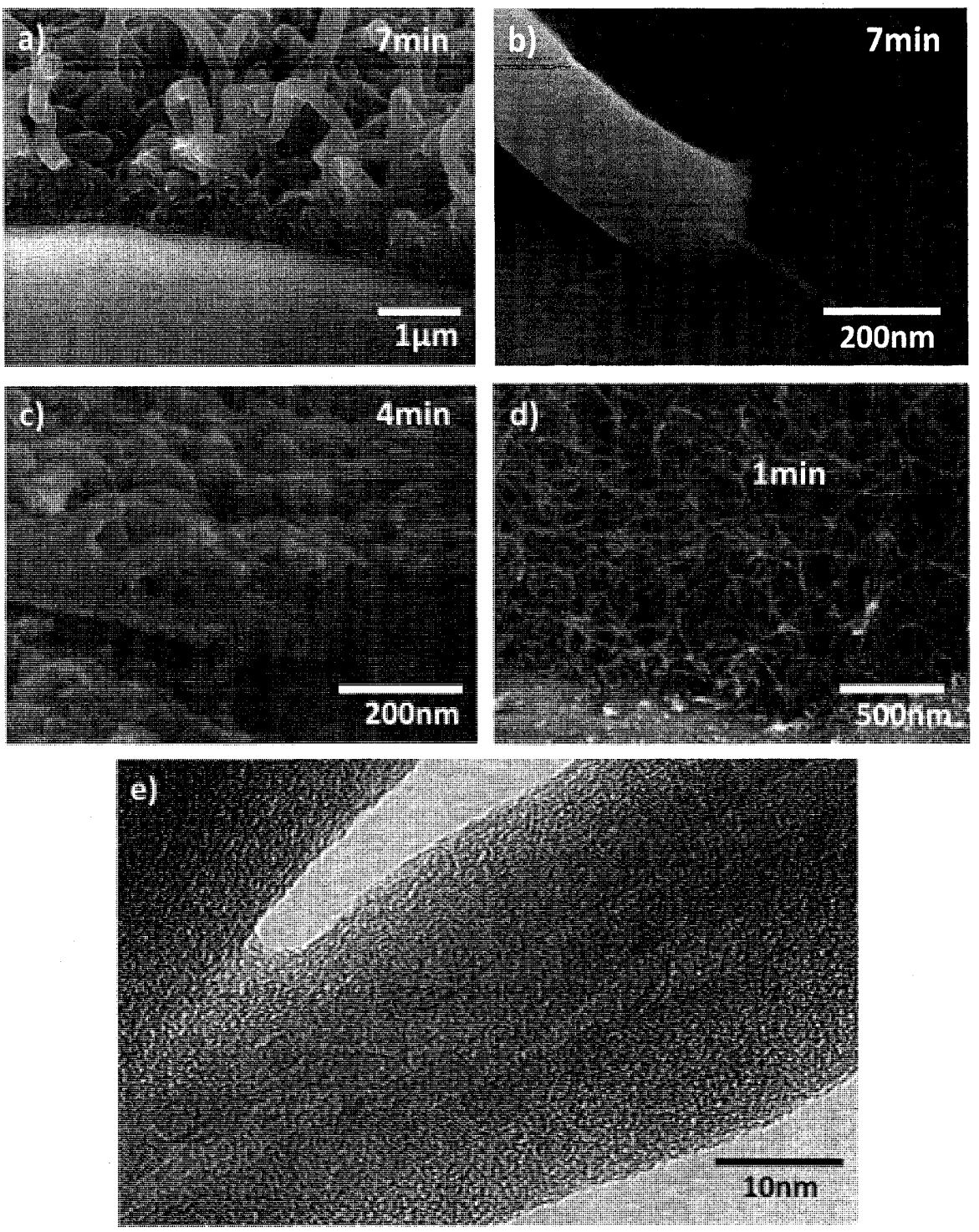

Figure 24: Effect of growth duration on CNT growth

Catalyst is Fe only. a) 7 min growth, b) broken CNT for 7 min growth, c) 4 min growth, d) 1 min growth without AC coverage, e) TEM of a CNT covered by AC.

When the growth time is reduced to 4 min while keeping the gas flow rates and temperature unchanged, the thickness of the AC base layer is reduced to around 250 nm from the 500 nm AC layer of the 7 min growth sample (Figure 24c). As the growth time is further reduced to 1 min (Figure 24d) the AC base layer entirely disappears and the amount of CNT grown is much greater than those from the longer growth runs. The greater amount of CNT grown and the lack of AC deposit with the 1 min growth mean that the carbon concentration never reached a level that leads to significant AC formation. Therefore growth duration can be used to limit AC formation.

The 4 min growth with Fe catalyst produces mostly AC while the 1min growth produces CNT in absence of AC. In comparison, at the same C_2H_4 flow rate the multilayered catalyst is able to handle at least 5 min of growth without any indication of AC formation. This suggests that the multilayered catalyst is able to process carbon at a much faster rate than Fe by itself. The increase carbon process rate reduces the amount of carbon available around the catalysts for AC formation. Therefore the multilayered catalyst is able to operate at higher carbon concentration, which further demonstrates its superiority over the Fe-only catalyst.

Another factor that affects the carbon concentration for AC formation and CNT growth is the growth temperature. At low growth temperature, carbon concentration is reduced. If the reduction rate in the rate of carbon uptake by the catalyst is less than the reduction in carbon concentration, then the catalysts are able to absorb higher portion of the carbon vapor surrounding the catalyst, leaving a reduced portion of carbon for AC formation. In this case, the CNT growth will continue longer and should obtain thicker VACNT film before AC poison the catalyst. Ultimately this depends heavily on the behavior of the catalyst. M. J. Bronikowski, during his experiment on VACNT growth at various temperatures, obtained surprising results where the VACNT is able to grow longer at lower temperature than it would at higher

temperature [74]. What Bronikowski observed can be explained by the simple concentration model established above.

Finally, the relative flow rate of carbon feedstock will have direct impact on the carbon concentration. To grow ultralong CNTs, a simple extension of the growth duration will not be the solution. Depending on the recipe and catalyst, prolonged gas release will move the gas concentration profile into equilibrium. In many cases, the carbon concentration at is too high and the catalysts are poisoned by AC before much CNT growth. One way to get around this is to reduce the carbon feedstock flow rate which decreases the carbon concentration at equilibrium. An alternative is to use a high carbon feedstock flow rate to rapidly ramp up the carbon concentration. Once carbon reaches a desired concentration, the process switches to a slower feedstock flow rate to maintain that concentration level. This way the growth process is able to operate at higher growth rate for longer duration to reduce total growth time required to reach target VACNT length.

5.5 When does CNT growth initiate?

When the carbon feedstock flow is stopped, there is still carbon present within the system for extended period of time, represented by the tail portion of the concentration time profile. CNT growth is not likely to stop at the point of the carbon feedstock gas cutoff. An experiment is conducted to study the effect of the tail portion of the concentration time profile on the CNT growth.

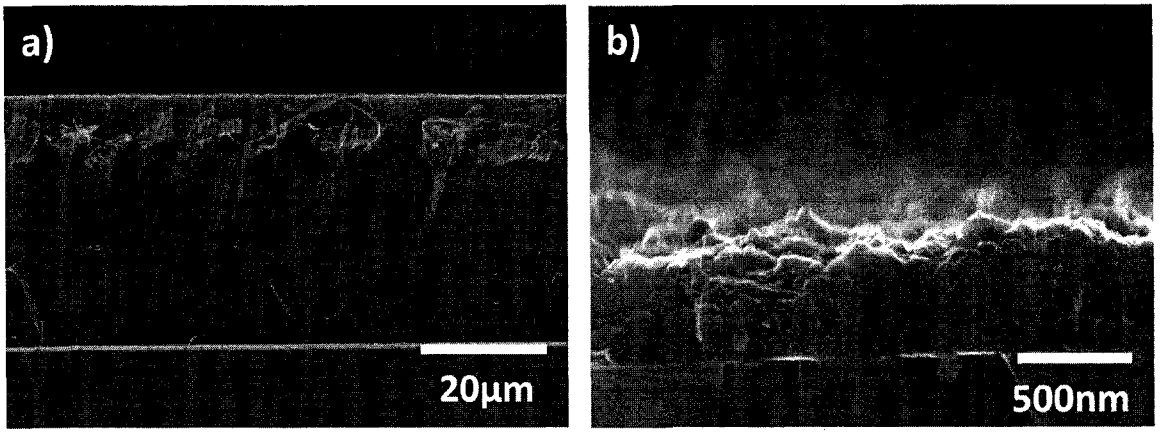

Figure 25: 5 min VACNT growth vs prolonged 30 min growth

Two back-to-back CNT growth runs are performed with the same catalyst (0.5 nm each for Fe, Ni, Cr, and 5 nm of Al_2O_3) under the same growth condition of 750°C and flow rates of 2500 sccm Ar, 300 sccm H_2 and 500 sccm C_2H_4. However, Sample 1 will undergo a growth step of 5 min, while Sample 2 will undergo an extended growth step of 30 min. The SEM images of the results are shown in Figure 25. Sample 1 produced 40 μm of dense VACNT. Both samples undergo exactly the same growth process until the 5 min mark of the growth step, where Sample 1 has its carbon feedstock cutoff while Sample 2 has its feedstock flow prolonged for an extra 25 min. If majority of VACNT growth on Sample 1 occurs during the 5 min of feedstock release, then there should also be VACNT present on Sample 2, though the VACNT may be cover by AC. However this is not the case. Figure 25b, shows the growth result of Sample 2. Neither clean VACNT nor AC covered VACNT are produced. Instead 500 nm of AC base layer is formed with scarce CNT growth. This means that the majority of VACNT growth on Sample 1 occurs after the feedstock cutoff. It seems that the catalyst undergoes several minutes of some process, currently unknown, in the presence of carbon feedstock before CNT growth actually initiates. (Figure 26)

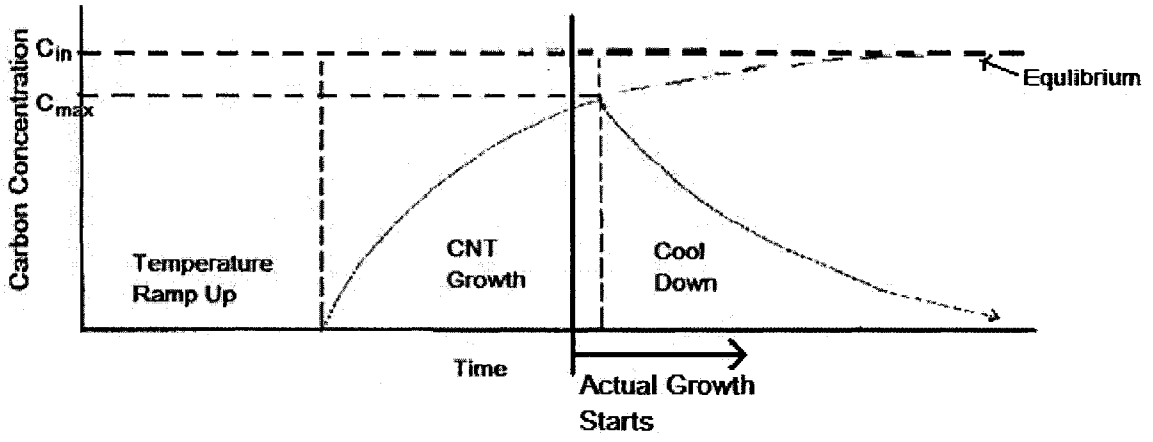

Figure 26: Graph of carbon concentration profile

CNT growth initiates in the latter portion of CNT growth step or later

With this mind, when describing an experiment or to quantify CNT growth, it is only accurate to state 5min of feedstock release at a certain flow rate rather than 5 min of CNT growth. This mistake is very common in the literature where the CNT growth rates are calculated. In those cases, the CNT growth rates are obtained by dividing the height of VACNT by the duration of feedstock release. From the evidence of the above experiment, CNT growth goes on for much longer after the feedstock has been shut off. In one of the extreme cases, the experiments used sub-1 sec feedstock release to obtain 100 μm of VACNT and concluded a growth rate of over 200 μm/s [75]. The claimed growth rate is orders of magnitude higher than the usual reported growth rate of between 10-100 μm/min. And most of VACNT growth likely occurs from the residue gas after the feedstock cutoff.

5.6 Local carbon concentration

The multilayered catalyst and established growth recipe using Tystar CVD is a novel high-volume process of growing CNT films. This technology is highly applicable to applications

such as field emission. In field emission, small bundles of VACNT are used as field emitters. In order to grow VACNTs in bundles, the catalysts need to be patterned into small catalyst pads.

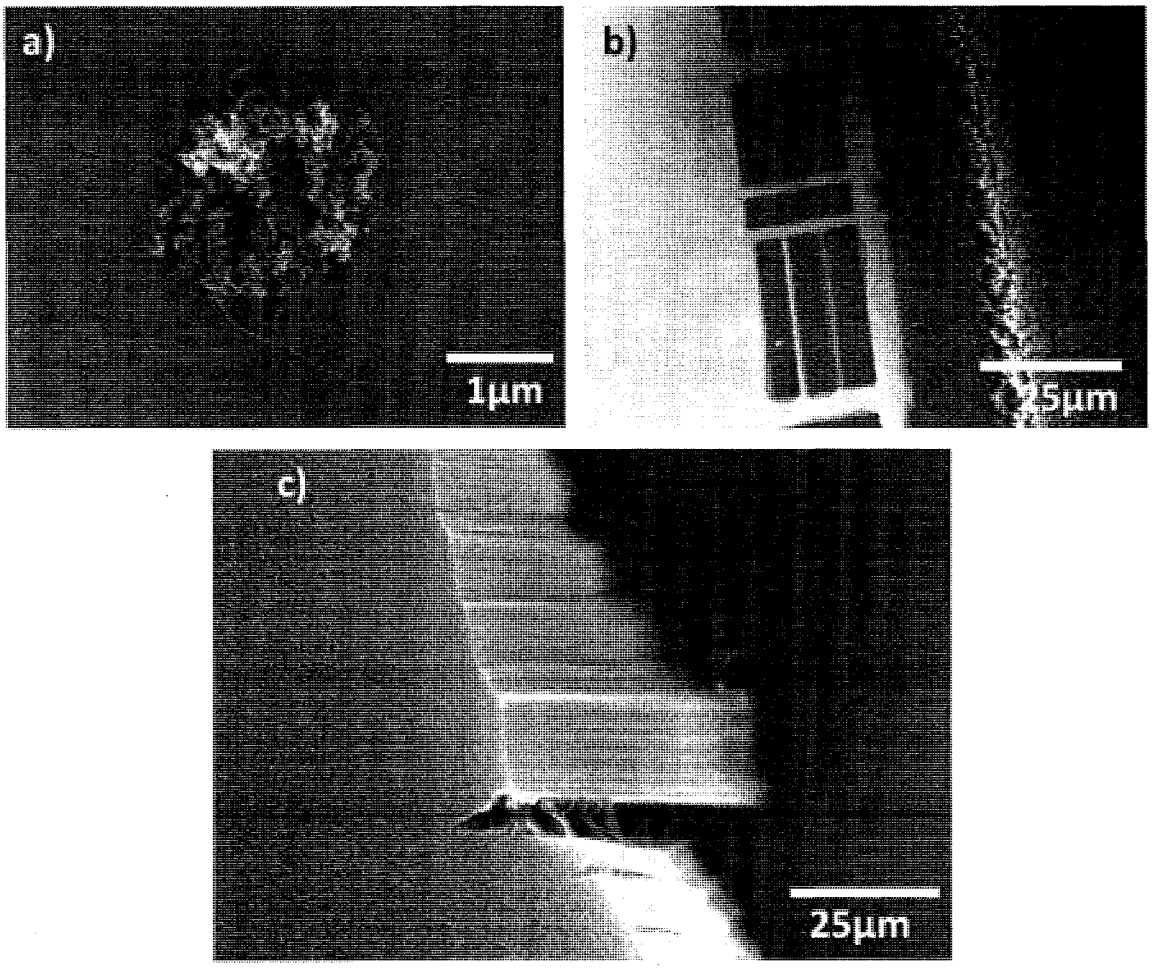

Figure 27: Local carbon concentration effect

a) no VACNT growth at 2 μm catalyst pads, b) no VACNT growth from small rectangles, thin VACNT growth from inner portion of the 2 mm large rectangle, c) massive VACNT growth at the center of the 2 mm large rectangle

Series of circular catalyst pads with diameters of 2 μm and larger rectangles of varying sizes are patterned using lithography and liftoff. The catalyst is composed of 5 nm Al_2O_3, 0.5 nm Cr, 0.1 nm Ni and 0.5 nm Fe deposited onto SiO_2 in the corresponding order using e-beam evaporation. The sample undergoes a growth step of 5min at 750°C with 2500 sccm Ar, 300

sccm H_2 and 500 sccm C_2H_4. The 2 μm circular catalyst pads (Figure 27a) and the smaller rectangles (Figure 27b) only have AC deposits and very small amount of CNT. For the large rectangle of 2 mm in width, the outer 15 μm of the edge has similar result of AC deposit, while VACNT growth only starts at inner portion of the rectangle. The VACNT film near the edge of the rectangle is relatively short at a few μm in height, whereas the height of VACNT film at the center of the rectangle is over 50 μm (Figure 27c). One way to explain the lack of CNT growth on small patterns and edges of large patterns is to consider the local carbon concentration at the immediate vicinity of the catalysts.

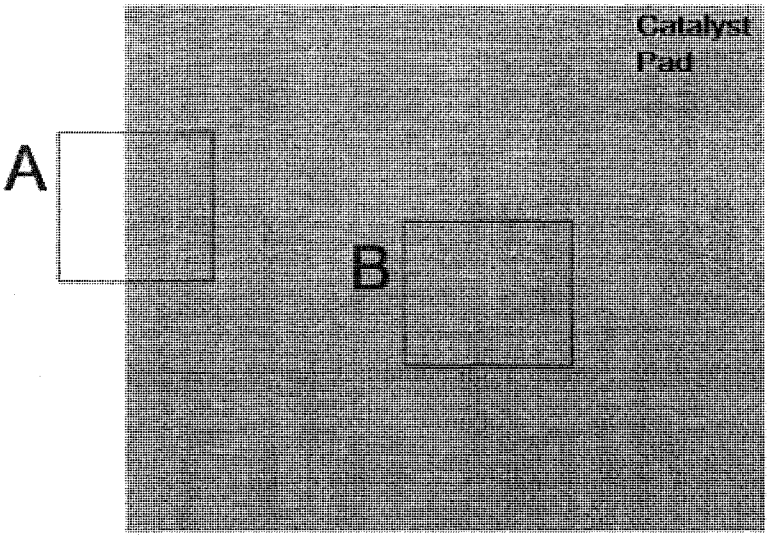

Figure 28: Local carbon concentration demonstration

There are fewer catalytic particles in the outer region (Figure 28) compared to the center of the catalyst pad. Therefore, the carbon consumption is lower at the edges of the pattern due to the lowered effective concentration of catalytic particles. Since the carbon consumption is lower, the carbon concentration at the immediate vicinity of theses catalysts is higher than that at the inner region of the large rectangle. This local carbon concentration will

decrease as the area of interest is moved towards the center of a large pattern away from the edges. In this experiment, the higher carbon concentration at the pattern edges puts the carbon level at a point where AC formation poisons the catalysts before much CNT growth can occur. At about 15 μm away from the pattern edge, the carbon concentration is reduced enough so that AC formation is slow enough to allow small amount of VACNT growth before completely poisons the catalysts. The center of the large rectangle is far enough from the edge of the rectangle so that the local carbon concentration is not affected by the areas without catalyst. CNT growth occurs as if the entire substrate surface is covered by catalytic particles where the Recipe and the Catalyst produce 10s of μm of VACNT as the case here. Iwasaki et al., grew VACNTs from holes of various sizes on SiO_2 [76]. They found the height of VACNT growth significantly decreases with the reduction in the hole sizes. The explanation given was the restricted carbon diffusion rate for the smaller holes. It could also due to the increase in the local carbon concentration for smaller feature sizes which leads to faster AC catalyst poisoning. Overall with the use of the Recipe and the Catalyst, minimum pattern size of 15 μm x 2 = 30 μm is required to have VACNT growth.

For field emission applications, the VACNT bundles may need to occupy smaller areas. Growing VACNT on smaller patterns can be achieved by lowering the overall carbon concentration through reducing the relative carbon feedstock flow rate, reducing the growth time or increasing the relative flow rate of H_2. Such experiment has not been carried out to test the local carbon concentration theory discussed above and should be investigated in future works.

5.7 Effect of H_2

The growth recipe contains flows of Ar, H_2 and C_2H_4. C_2H_4 has been extensively discussed in the earlier sections and Ar is the carrier gas. The role that H_2 plays during CNT growth is not clear. The pyrolysis of C_2H_4 is very complex involving many kinds of C_2H_x molecules [77]. However, the net reaction is

$$C_2H_4 \leftrightarrow 2C + 2H_2$$

The presence of H_2 flow increases the H_2 concentration in the furnace and biases the reaction towards C_2H_4 formation. The consequence is the reduction of carbon concentration. And by this reasoning, H_2 can be used as another parameter to regulate carbon concentration - the higher the H_2 flow rates, the lower the carbon concentration. H_2 also interacts with CNT sidewalls and can etch CNTs at high enough temperature and H_2 concentration [78]. The surface defects of CNT are more prone to etching as they do not have a stable graphite structure, so the H_2 etching may help decrease defect concentration on CNTs and improve CNT quality CNT [78,79].

Dai et al. has performed several experiments with H_2 and observed no significant effect on CNT growth [78]. He is able to grow similar SWNTs with H_2 and also without H_2 in PECVD. However, high dosage of H_2 etches SWNTs. No experiments on H_2 have been performed for this project and should be looked into in the future to improve CNT growth.

6 Further Directions

A multilayered catalyst and growth recipe are established on Tystar CVD to grow long and dense VACNTs. However, there is still large room for improvements and many concepts to explore and understand.

6.1 Extended Growth

The multilayered catalyst shows great potential as the catalyst to carry out further carbon nanotube research. The large amount of VACNT grown in short time using the multilayered catalyst suggests the catalyst can process carbon rapidly and operate with large tolerance on the growth environment. To explore into the full potential of the catalyst, extended VACNT growth using either reduced carbon feedstock flow rate or the two stage growth should be look into. Ultralong VACNTs will see applications in material composites to improve strength, and replacing carbon fiber as the new light weight high strength material.

6.2 Growth on Small Catalyst Pads

To study and verify the local carbon concentration theory, reduction of carbon feedstock flow rate or growth duration can be attempted to grow VACNT on small catalyst

patterns. Application wise, these experiment are also part of the process towards the fabrication of small scale CNT field emitters.

6.3 Uniformity

In order to mass produce CNT, especially CNT devices, the CNT growth uniformity across substrate surface or multiple substrates is an important factor. Currently, experiments placing the sample substrate perpendicular to gas flow and in between two dummy substrates to simulate multiwafer process does yield great growth uniformity across the entire wafer with much greater VACNT growth at the wafer edge than at the center. Better uniformity is achieved by placing the substrate parallel to gas flow in the furnace, but this type of substrate placement drastically reduces the load capability of the Tystar CVD from 50 substrates/run to 4 substrates/run. To improve the uniformity for vertical substrate placement, LPCVD can be used to reduce the length of the boundary layer.

6.4 Catalyst Pre-growth Treatment

One crucial step of CNT growth that has not been studied in this project is the catalyst pre-growth treatment. The catalyst pre-growth anneal step used in this project corresponds to the temperature ramp up step of the CNT growth process, and is thus not directly manipulated or studied. Many literatures have paid great attention to the pre-growth treatment using separate anneal step, different anneal gas, and etc [46]. Future experiments can certainly focus on catalyst pre-growth treatment using a separate anneal step using different temperature and anneal length. The amount of H_2 flow during the temperature ramp up step can be varied to see their effects on CNT growth. This pre-growth treatment step is expected to have significant influence on the quality of CNTs.

6.5 Water Assisted Growth

Water is a mild oxidizing agent. Many literatures have confirmed that water etches AC and CNT defects, while leaving the quality CNTs untouched if the water concentration is at the right level. The experiments conducted during this project have not explored into the use of water vapor during CNT growth. However, the Tystar CVD has the capability of injecting water vapor into the growth chamber and the use of water should improve both the catalytic activity of the catalysts and the quality of CNTs.

6.6 Residual Gas Analyzer

Finally, if a residual gas analyzer (RGA) is installed on the Tystar CVD, it can be used to gain more insight into the chemical reactions that happen within the furnace. Qualitatively, RGA reveals the identities of every gas that are present or formed during CNT growth process. Quantitatively, RGA tells us the degree of ethylene pyrolysis at growth condition by monitoring the amount of carbon atoms that go through the exhaust, and also the rate of carbon consumption from the net difference of carbon input and carbon exhaust.

7 Conclusion

A novel multilayered catalyst of 5 nm Al_2O_3, 0.5 nm Cr, 0.1 nm Ni and 0.5 nm Fe deposited onto SiO_2 surface is used to grow long and dense VACNTs using ethylene as carbon feedstock in a high volume Tystar CVD system. The longest VACNT grown in 5 min of ethylene release is 160 μm. This technology establishes a high-volume process for carbon nanotube film production.

The composition of the catalyst has been found to be highly influential in catalyst performance leading to VACNT growth. 5 nm of Al_2O_3 provides the best VACNT growth in terms of VACNT thickness. Al_2O_3 acts as a separation layer between the catalyst and the substrate surface, and it may also interact with catalyst materials to restrict their movement leadings to smaller catalytic particle sizes. Cr does not get incorporated into the catalyst during CNT growth. The role of Cr is to form an underlayer that interacts with the Fe-Ni catalyst to improve their catalytic performance, such as the ability to process and dissociate ethylene into carbon atoms. Cr may also shapes catalyst movement at high temperature to prevent catalyst agglomeration into larger particles. Fe and Ni are found to be the elements that catalyze CNT growth. A high Fe:Ni thickness ratio is ideal for long VACNT growth. The mechanism behind the improved catalyst performance at high Fe:Ni thickness ratio may be due to the better structural suitability of the BCC αFe,Ni phase towards carbon processing leading to CNT growth.

During the CNT growth, it is very important to regulate carbon concentration to prevent AC formation. AC poisons catalysts and stops their catalytic functions. The large process chamber in the Tystar CVD requires more than 8 min from the initial release of carbon feedstock until all gases to reach concentration equilibrium. For short growth duration of several minutes, the longer the growth length is, the higher the level of carbon concentration can be reached during the process. Depending on the catalyst design and the growth environment such as the temperature, the growth length should be regulated so that the carbon concentration never reaches a level to cause significant AC formation. VACNT growth is found to initiate at the later portion of the growth step, while having majority of the growth occur after the carbon feedstock flow has been shut-off. Local carbon concentrations at the immediate vicinity of catalysts have significant effect on the growth in the region. For patterned catalyst pads, the closer the catalyst is to the edge, the lesser the number of catalysts are in the surrounding area to consume carbon. Hence the local carbon concentration increases and may poison the catalysts before VACNT growth. The smallest catalyst pattern to produce VACNT growth using the Catalyst and the Recipe needs to be at least 30 μm in thinnest part of the pattern. The concentration model and local concentration theory developed in this thesis can explain several unexplained CNT growth phenomena mentioned in many publications.

There is still much room for further study and optimization of the CNT growth process on Tystar CVD. Extended growth should be performed to examine the full potential of the multi-layered catalyst and to see how long these VACNTs can grow before limited feedstock access to the catalyst and graduate AC poisoning of the catalysts stop the growth. Further experiments can examine and establish a suitable condition using water vapor during the CNT growth step to further reduce AC formation and improve CNT quality. The catalyst pre-growth treatment should be looked into to understand the precise effects of the parameters in pre-growth

treatment. Experimenting with catalyst pre-growth treatment may lead to significant breakthrough or improvements in the resulting grown CNTs. And finally, experiments using reduced carbon feedstock flow, reduced temperature, or reduce growth length can be carried out to test the local carbon concentration theory and to establish the growth parameters to grow VACNT on small catalyst pads which are applicable towards incorporation of VACNT into miniature devices. The VACNT growth technology established in this thesis can be used as the basis towards researches into suitable applications, such as field emission, field effect transistor, hydrogen storage and advanced composite material. The catalyst design and growth recipe can be further tuned and optimized to suit the application of interest.

Despite years of research into controlling CNT growth, current technology still mainly offers only random selection of CNT size, type, direction, within a fairly large range outside the tolerance of the intricate applications that CNTs hold great promises for. One way to get around this is to build devices incorporating bundles or groups of CNTs. The VACNT growth technology described in this thesis can produce CNT bundles in high volume to use in CNT devices. These devices will be designed based on the bundled properties of CNTs. The effective material properties of CNT bundles will be much less sensitive to the randomness in CNT, which can greatly improve device yield. Also VACNT provides directional growth without external aids. Therefore at the current stage, applications that employ groups of CNTs such as energy storage, field emission displays and composite materials are the most promising direction towards CNT commercialization. As CNT growth technology matures further, intricate CNTFET transistors may be then incorporated into mass produced consumer products.

References

[1] Sakintunaa, B., Darkrimb, F. L. and Hirscher, M., *Metal hydride materials for solid hydrogen storage: A review,* Int. J. Hydrogen Energ., vol. 32, pp.1121-40, 2007.

[2] MacDonald, B. and Rowe, A. M., *A thermally coupled metal hydride hydrogen storage and fuel cell system,* J. Power Sources, vol.161, pp.346-55, 2006.

[3] Galhano, G. A., Melo R. M. and Bottino, M. A., *Evaluation of the Flexural Strength of Carbon Fiber-, Quartz Fiber-, and Glass Fiber-Based Posts*, J. Endodont., vol.31, pp.209-11, 2005.

[4] Chianella, I., Karima, K. and Piletska, E. V., *Computational design and synthesis of molecularly imprinted polymers with high binding capacity for pharmaceutical applications-model case: Adsorbent for abacavir*, Analytica Chimica Acta, vol.559, pp.73-8, 2006.

[5] Ulbrich, T. C., Makarov, D., Hu, G., Guhr, I.L., Suess, D., Schrefl, T. and Albrecht, M., *Magnetization reversal in a novel gradient nanomaterial*, Phys. Rev. Lett., vol.96, 077202, 2006.

[6] Ogawa, K., Aoki, N., Miyazawa, K., Nakamura, S., Mashino, T., Bird, J.P. and Ochiai, Y., *C60 nanowhisker field-effect transistor application for nano-electronics*, Jpn. J. App. Phys., vol.47, pp.501-4, 2008.

[7] Xu, J., Zhou, J., Yao, Y., Cen, Z., Song, F., Xu, L., Wan, J., and Chen, K., *Enhanced electron field emission from dense Si nano-dots prepared by laser crystallization of ultrathin amorphous Si films*, Solid State Commun., vol.145, pp.433-6, 2008.

[8]Iijima, S., *Helical microtubules of graphitic carbon*, Nature, vol.354, pp56-8, 1991.

[9] Li, J., Ye, Q., Cassell, A., Ng, H. T., Stevens, R., Han, J., and Meyyappan, M., *Bottom-up approach for carbon nanotube interconnects*, Appl. Phys. Lett., vol.82, pp.2491-3, 2003.

[10] Anatram, M.P., and L'eonard, F., *Physics of carbon nanotube electronic devices,* Rep. Prog. Phys., vol.69, pp.507-61, 2006.

[11] Srivastava, N., and Banerjee, K., *Performance Analysis of Carbon Nanotube Interconnects for VLSI Applications*, Proceedings of the 2005 IEEE/ACM International conference on Computer-aided design, pp.383-390, 2005.

[12] Qin, Z., Feng, X.Q., Zou, J., Yin, Y., and Yu, S.W., *Superior flexibility of super carbon nanotubes: Molecular dynamics simulations*, Appl. Phys. Lett., vol.91, 043108, 2007.

[13] Kim, S.K., Xuan, Y., Ye, P.D., Mohammadi, S., Back, J.H., and Shim, M., *Atomic layer deposited Al_2O_3 for gate dielectric and passivation layer of single-walled carbon nanotube transistors*, Appl. Phys. Lett., vol.90, 163108, 2007.

[14] Liu, C., Yong, Y., Cheng, H.M., Golberg, D., and Bando, Y., *Field emission properties of macroscopic single-walled carbon nanotube* strands, Appl. Phys. Lett., vol.86, 223114, 2005.

[15] Li, I. L. and Tang, Z.K., *Curvature effect in ultra-small single-walled carbon nanotubes*, Appl. Surf. Sci., vol. 226, pp.72-7, 2004.

[16] Wang, N., Tang, Z. K., Li, G. D. and Chen, J. S., *Single-walled 4Å carbon nanotube arrays*, Nature, vol.408, pp.50-1, 2000.

[17] S. Reich, C. Thomsen and J. Maultzsch, *Carbon Nanotubes: Basic Concepts and Physical Properties*, Weinheim, Wiley-VCH, 2004.

[18] Kunstmann, J., Quandt, A., and Boustani, I., *An approach to control the radius and the chirality of nanotubes,* Nanotechnology, vol.18, 155703, 2007.

[19]Son, Y.W., Ihm, J., Cohen, M.L., Louie, S.G., and Choi, H.J., *Electrical Switching in Metallic Carbon Nanotubes*, Phys. Rev. Lett., vol.95, 216602, 2005.

[20] Andoa, T., Matsumuraa, H., Nakanishi, T., *Theory of ballistic transport in carbon nanotubes*, Physica B, vol.323, pp.44-50, 2002.

[21] Park, J.Y., Rosenblatt, S., Yaish, Y., Sazonova, V., Braig, H. S., Arias, T. A., Brouwer, P. W., and McEuen, P. L., *Electron-phonon scattering in metallic single-walled carbon nanotubes*, Nano lett., vol.4, pp.517-20, 2004.

[22] O'Connell, M.J., *Carbon Nanotubes: Properties and Applications*, Boca Raton, Taylor & Francis Group, 2006.

[23] Wildoer, J. W. G., Venema, L. C., Rinzler, A. G., Smalley, R. E., and Dekker, C., *Electronic structure of atomically resolved carbon nanotubes*, Nature, vol.391, pp.59-62, 1998.

[24] Odom, T. W., Huang, J. L., Kim, P., Lieber, C. M., *Atomic structure and electronic properties of single-walled carbon nanotubes*, Nature, vol.391, pp.62-4, 1998.

[25] Tans, S. J., Verschueren, A. R. M., and Dekker, C., *Room-temperature transistor based on a single carbon nanotube*, Nature, vol.393, pp.49-52, 1998.

[26] Martel, R., Schmidt, T., Shea, H. R., Hertel, T., and Avourisa, P., *Single- and multi-wall carbon nanotube field-effect transistors*, Appl. Phys. Lett., vol.73, pp.2447-9, 1998.

[27] Radosavljevic, M., Appenzeller, J., Avourisc, P., and Knoch, J., *High performance of potassium n-doped carbon nanotube field-effect transistors*, Appl. Phys. Lett., vol.84, pp.3693-5, 2004.

[28] Saito, Y., and Uemura, S., *Field emission from carbon nanotubes and its application to electron source*, Carbon, vol.38, pp.169-82, 2000.

[29] Bonard, J.M., Kind, H., Stockli, T., and Nilsson, L.O., *Field emission from carbon nanotubes: the first five years*, Solid State Electron., vol.45, pp.893-914, 2001.

[30] Bachilo, S.M., Strano, M. S., Kittrell, C., Hauge, R. H., Smalley, R. E. and Weisman, R. B., *Structure-assigned optical spectra of single-walled carbon nanotubes*, Science, vol.298, pp.2361-6, 2002.

[31] Hatschuh, A., Pedrosa, H. N., Novotny, L., and Krauss, T. D., *Simultaneous fluorescence and Raman scattering in single carbon nanotubes*, Science, vol.301, pp.1354-6, 2003.

[32] Hagen, A., and Hertel, T., *Quantitative analysis of optical spectra from individual single-wall carbon nanotubes*, Nano Lett., vol.3, pp.383-8, 2003.

[33] Lefebvre, J., Homma, Y., and Finnie, P., *Bright band gap photoluminescence from unprocessed single-walled carbon nanotubes*, Phys. Rev. Lett., vol.90, 217401, 2003.

[34] Misewich, J. A., Martel, R., Avouris, P., Tsang, J. C., Heinze, S., Tersoff, J., *Electrically induced optical emission from a carbon nanotube FET*, Science, vol.300, pp.783-6, 2003.

[35] deHeer, W. A., Bacsa, W. S., Chatelain, A., Gerfin, T., Humphrey-Baker, R., Forro, L., and Ugarte, D., *Aligned carbon nanotube films: production and optical and electronic properties*, Science, vol.268, pp.845-7, 1995.

[36] Meyyappan, M., *Carbon nanotubes: science and applications*, Boca Raton, CRC Press, 2005.

[37] Fantini, C., Jorio, A., Souza, M., Strano, M.S., Dresselhaus, M.S., and Pimenta, M.A., *Optical Transition Energies for Carbon Nanotubes from Resonant Raman Spectroscopy: Environment and Temperature Effects*, Phys. Rev. Lett., vol.93, 147406, 2004.

[38] Henrard, L., Loiseau, A., Journet, C., and Bernier, P., *Study of the symmetry of single-walled nanotubes by electron diffraction*, Eur. Phys. J. B, vol.13, pp.661-70, 2000.

[39] Yu, M.F., Files, B.S., Arepalli, S., and Ruoff, R.S., *Tensile Loading of Ropes of SingleWall Carbon Nanotubes and their Mechanical Properties*, Phys. Rev. Lett., vol.84, pp.5552-5, 2000.

[40] Loiseau, A., Launois, P., Petit, P., Roche, S., and Salvetat, J. P., *Understanding Carbon Nanotubes*, Berlin, Springer, 2006.

[41] Yao, N., and Lordi, V., *Young's Modulus of single-walled carbon nanotubes*, J. Appl. Phys., vol.84, pp.1939-43, 1998.

[42] Wei, C., Cho, K., and Srivastava, D., *Tensile strength of carbon nanotubes under realistic temperature and strain rate*, Phys. Rev. B, vol.67, 115407, 2003.

[43] Salvetat, J.P., Kulik, A.J., Bonard, J.M., Briggs, G.D., Stockli, T., Motonier, K., Bonnamy, S., Boguin, F., Burnham, N., and Forro, L., *Elastic Modulus of Ordered and Disordered Multiwalled Carbon Nanotubes*, Adv. Mater., vol.11, pp.161-5, 1999.

[44] Suekane, O., Nagasaka, T., Kiyotaki, K., and Nosaka, T. *Rapid Growth of Vertically Aligned Carbon Nanotubes*, Jpn. J. Appl. Phys., vol.43, pp.1214-6, 2004.

[45] Huha, Y., Lee, J.Y., and Lee, C.J., *Growth of vertically aligned carbon nanotube emitters on patterned silicon trenches for field emission applications*, Thin Solid Films, vol.475, pp.267-70, 2005.

[46] Yoshihara, K., Honda, S., Lee, J.G., Mori, H., and Oura, K., *High-Density Growth of Vertically Aligned Carbon Nanotubes with High Linearity by Catalyst Preheating in Acetylene Atmosphere*, Jpn. J. Appl. Phys., vol.47, pp.1941-3, 2008.

[47] Hata, K., Futaba, D.N., Mizuno, K., Namai, T, Yumura, M., and Iijima, S., *Water-Assisted Highly Efficient Synthesis of Impurity-Free Single-Walled Carbon Nanotubes*, Science, vol.306, pp.1362-4, 2004.

[48] Jang, J.E., Cha, S.N., Choi, Y., Amaratungab, G.A.J., Kang, D.J., Hasko, D.G., Jung, J.E., and Kim, J.M., *Nanoelectromechanical switches with vertically aligned carbon nanotubes*, Appl. Phys. Lett., vol.87, 163114, 2005.

[49] Zhong, G., Iwasaki, T., Honda, K., Furukawa, Y., Ohdomari, I., and Kawarada, H., *Low Temperature Synthesis of Extremely Dense and Vertically Aligned Single-walled carbon nanotubes*, Jpn. J. Appl. Phys., vol.44, pp.1558-61, 2005.

[50] Keidar, M., *Factors affecting synthesis of single wall carbon nanotubes in arc discharge*, J. Phys. D Appl. Phys., vol.40, pp.2388-93, 2007.

[51] Nga, L.T., Bonard, J.M., Gaal, R., Forro, L., and Hernadi, K., *Comparison of catalytically grown and arc-discharge carbon nanotube tips,* Appl. Phys. Lett., vol.80, pp.850-2, 2002.

[52] Guo, T., Nikolaev, P., Rinzler, A.G., Tomanek, D., Colbert, D.T., and Smalley, R.E., *Self-Assembly of Tubular Fullerenes,* J. Phys. Chem., vol.99, pp.10694-7, 1995.

[53] Scott, C.D., Arepall, S., Nikolaev, P., and Smalley, R.E., *Growth mechanisms for single-wall carbon nanotubes in a laser-ablation process*, Appl. Phys. A-Mater., vol.72, pp.573-80, 2001.

[54] Lacerda, R.G., The, A.S., Yang, M.H., Teo, K.B.K., Lupesinghe, N.L., Dala, S.H., Koziol, K.K.K., Roy, D., Amaratunga, G.A.J., Milne, W.I., Chhowalla, M., Hasko, D.G., Wyczisk, F., and Legagmeux, P., *Growth of high-quality single-wall carbon nanotubes without amorphous carbon formation*, Appl. Phys. Lett., vol.84, pp.269-271, 2004.

[55] Gaillard, J., Skove, M., and Rao, A.M., *Mechanical Properties of CVD Grown Multi-walled Carbon Nanotubes,* Mater. Res. Soc. Symp. Proc., Vol.858E, 2005.

[56] Vajtai, R., Wei, B.Q., and Ajayan, P.M., *Controlled growth of carbon nanotubes*, Phil. Trans. R. Soc. Lond. A, vol.362, pp.2143-60, 2004.

[57] Li, Y, Zhang, X.B., Tao, X.Y., Xu, J.M., Huang, W.Z, Luo, J.H., Luo Z.Q., Li, T., Liu, F., Bao, Y., and Geise, H.J., *Mass production of high-quality multi-walled carbon nanotube bundles on a Ni/Mo/MgO catalyst*, Carbon, vol.43, pp.295-301, 2005.

[58] Wang, Y., Luo, Z., Li, B., Ho, P.S., Yao, Z., Shi, L., Bryan, E.N., and Nemanich, R. J., *Comparison study of catalyst nanoparticle formation and carbon nanotube growth: Support effect*, J. Appl. Phys., vol.101, 124310, 2007.

[59] Avouris, P., Appenzeller, J., Martel, R., and Wind, S., *Carbon Nanotube Electronics*, P. IEEE, vol.91,pp.1772-84,2003.

[60] Nikitin, A., Li, X., Zhang, Z., Ogasawara, H., Dai, H., and Nilsson, A., *Hydrogen Storage in Carbon Nanotubes through the Formation of Stable C–H Bonds*, Nano Lett., vol.8, pp.162-7, 2008.

[61] Zhang, G., Mann, D., Zhang, L., Javey, A., Li, Y., Yenilmez, E., Wang, Q., McVitie, J.P., Nishi, Y., Gibbons, J., and Dai, H., *Ultra-high-yield growth of vertical single-walled carbon nanotubes: Hidden roles of hydrogen and oxygen*, PNAS, vol.102, pp.16141-5, 2005.

[62] Cassel, M., Verma, S., Delzeit, L., Meyyappan, M., and Han, J., *Combinatorial Optimization of Heterogeneous Catalysts Used in the Growth of Carbon Nanotubes*, Langmuir, vol.17, pp.260-4, 2001.

[63] Choi, H.C., Kim, W., Wang. D., and Dai, H., *Delivery of Catalytic Metal Species onto Surfaces with Dendrimer Carriers for the Synthesis of Carbon Nanotubes with Narrow Diameter Distribution*, J. Phys. Chem. B, vol.106, pp.12361-5, 2002.

[64] Mohamed, G.H., *MEMS: Design and fabrication: the MEMS Handbook*, Boca Raton, Taylor & Francis, 2006.

[65] Yang, T.Y., Yang, W.C., Tseng, T.C., Tsai, C.M., and Yewa, T.R., *Ni–Cr alloy to enhance single- and double-walled carbon nanotube synthesis for field-effect transistor fabrication*, Appl. Phys. Lett., vol.90, 223103, 2007.

[66] Jung, Y.J., Wei, B., Vajtai, R., Ajayan, P.M., Homma, Y., Prabhakaran, K., and Ogino, T., *Mechanism of Selective Growth of Carbon Nanotubes on SiO2/Si Patterns*, Nano Lett., vol.3, pp.561-4, 2003.

[67] Nolan, P.E., Lynch, D.C., and Cutler, A.H., *Carbon Deposition and Hydrocarbon Formation on Group VIII Metal Catalysts*, J. Phys. Chem. B, vol.102, pp.4165-75, 1998.

[68]Tung, S.E., Mcininch, E., *High purity alumina III: Ion radical cracking of cumene on alumina,* J. Catal., vol.4, pp.586-93, 1965.

[69] Dallaporta, H., Liehr, M., and Lewis, J.E., *Silicon dioxide defects induced by metal impurities,* Phys. Rev. B, vol.41, pp.5075-83, 1992.

[70] MacIver, D.S., Wilmot, W.H., and Bridges, J.M., *Catalytic aluminas: II. Catalytic properties of eta and gamma alumina,* J. Catal., vol.3 pp.502-11, 1964.

[71] Hasegawa, K., Sugime, H., Kakehi, K., Zhang, Z., Maruyama, S., and Yamaguchi, Y., *Millimeter-Thick Single-Walled Carbon Nanotube Forests: Hidden Role of Catalyst Support*, Jpn. J. Appl. Phys., vol.46, pp.399-401, 2007.

[72] Arcos, T., Garnier, M.G., Oelhafen, P., Mathys, D., Seo, J.W., Domingo, C., Garcia-Ramos, J.V., and Cortes, S.S., *Strong influence of buffer layer type on carbon nanotube characteristics*, Carbon, vol.42, pp.187-90, 2004.

[73] ASM, *ASM Handbook volume 3: Alloy Phase Diagrams*, ASM International, 1992.

[74] Bronikowski, M. J., *Longer Nanotubes at Lower Temperatures: The influence of effective activation energies on carbon nanotube growth by thermal chemical vapor deposition,* J. Phys. Chem. C, vol.111, pp.17705-12, 2007.

[75] Suekane, O., Nagasaka, T., Kiyotaki, K., Nosaka, T., and Nakayama, Y., *Rapid growth of vertically aligned carbon nanotubes*, Jpn. J. Appl. Phys., vol.43, pp.1214-6, 2004.

[76] Iwasaki, T., Morikane, R., Edura, T., Tokuda, M., Tsutsui, K., Wada, Y. and Kawarada H., *Growth of dense single-walled carbon nanotubes in nano-sized silicon dioixide holes for future microelectronics*, Carbon, vol.45, pp.2351-5, 2007.

[77] Hidaka, Y., Nishimori, T., Sato, K., Henmi, Y., Okuda, R., Inami, K., and Higashihara, T., *Shock-Tube and Modeling Study of Ethylene Pyrolysis and Oxidation*, Combust. Flame, vol.117, pp.755-76, 1999.

[78] Zhang, G., Qi, P., Wang, X., Lu, Y., Mann, D., Li, X., and Dai, H., *Hydrogenation and Hydrocarbonation and Etching of Single-Walled Carbon Nanotubes*, J. Am. Chem. Soc., vol.128, pp.6026-7, 2006.

[79] Nikitin, A., Ogasawara, H., Mann, D., Denecke, R., Zhang, Z., Dai, H., Cho, K., and Nilsson, A., *Hydrogenation of Single-Walled Carbon Nanotubes*, Phys. Rev. Lett., vol.95, 225507, 2005.